Oxo Complexes, pH Effects, and Catalysis in Films Formed by Electropolymerization†

Ana R. Guadalupe, Xiaohong Chen, B. Patrick Sullivan, and Thomas J. Meyer*

Kenan and Venable Laboratories, Department of Chemistry, The University of North Carolina at Chapel Hill, Chapel Hill, North Carolina 27599-3290

Received June 16, 1993®

Electrodes coated with thin polymeric films of $^1/_3$poly-*cis*-$[Ru(vbpy)_2(H_2O)_2]^{2+}$-*co*-$^2/_3$poly-$[Ru(vbpy)_3]^{2+}$(vbpy is 4-methyl-4′-vinyl-2,2′-bipyridine) or poly-*cis*-$[Ru(pyr\text{-}bpy)_2(H_2O)_2]^{2+}$ (pyr-bpy is 4-(2-pyrrol-1-yl-ethyl)-4′-methyl-2,2′-bipyridine) have been prepared and characterized by electrochemical and spectroscopic measurements. Stepwise aquation of the precursor, poly-*cis*-$[Ru(pyr\text{-}bpy)_2Cl_2]$, occurs, but only after oxidative excursions through the $Ru^{III/II}$ wave. Acid-induced aquation of poly-*cis*-$[Ru(pyr\text{-}bpy)_2(CO_3)]$ to give the corresponding diaqua complex also occurs, through a detectable bicarbonato intermediate. Similarly, addition of acid to polymeric films of $^1/_3$poly-$[Ru(vbpy)_2(CO_3)]$-*co*-$^2/_3$poly-$[Ru(vbpy)_3]^{2+}$ leads to $^1/_3$poly-*cis*-$[Ru(vbpy)_2(H_2O)_2]^{2+}$-*co*-$^2/_3$poly-$[Ru(vbpy)_3]^{2+}$. Waves appear in cyclic voltammograms of the films containing aqua complexes attributable to $Ru^{III/II}$, $Ru^{IV/III}$, $Ru^{V/IV}$, and $Ru^{VI/V}$ couples analogous to those observed for *cis*-$[Ru(bpy)_2(H_2O)_2]^{2+}$ in solution. The film-based couples are pH dependent as expected because of the increased acidity on oxidation, e.g., poly-*cis*-$[Ru^{II}(pyr\text{-}bpy)_2(H_2O)_2]^{2+} \rightarrow$ poly-*cis*-$[Ru^{III}(pyr\text{-}bpy)_2(OH)(H_2O)]^{2+} + e + H^+$. The electron-transport properties of the films are medium and time dependent. Peak currents for the higher oxidation state couples decrease after the first voltammetric scan. In poly-*cis*-$[Ru(pyr\text{-}bpy)_2(H_2O)_2]^{2+}$, peak currents for the $Ru^{III/II}$ couple decrease as the pH is increased from 1.2 to 11.9. In solution, oxidation of *cis*-$[Ru^{II}(bpy)_2(H_2O)_2]^{2+}$ to *cis*-$[Ru^{VI}(bpy)_2(O)_2]^{2+}$ leads to decomposition by loss of bpy to give *trans*-$[Ru^{VI}(bpy)(O)_2(OH)_2]$. This reaction appears to be inhibited in the film, and Ru^{VI} is stabilized. Preliminary studies have been made of the electrocatalytic oxidation of benzyl alcohol and of chloride ion by poly-*cis*-$[Ru(pyr\text{-}bpy)_2(H_2O)_2]^{2+}$ by rotating-disk voltammetry. Catalysis of both oxidations occurs in potential regions associated with the $Ru^{V/IV}$ or $Ru^{VI/V}$ couples. The mechanism for the oxidation of benzyl alcohol appears to be related to that for $[Ru(bpy)_2(py)(O)]^{2+}$ as oxidant in solution as demonstrated by a $C_6H_5CH_2OH/C_6H_5CD_2OH$ kinetic isotope effect of ≥29.

Introduction

Electrochemical methods can offer an attractive alternative to chemical oxidation or reduction in organic or inorganic synthesis.[1] In principle, the development of chemically modified electrodes provides a means for improving the performance of solid electrodes by incorporating catalytic sites at the electrode–solution interface. These can act as molecular interfaces meeting the mechanistic demands of the reaction of interest while undergoing electron transfer with the electrode.[2] Some of the advantages of this approach are that (1) an active and selective catalyst can be designed based on solution studies, (2) the amount of catalyst required is low, and (3) the catalyst is confined to the interface where the net reaction occurs.

Polypyridyl complexes of ruthenium and osmium can act as catalysts or stoichiometric reagents for the oxidation of organic and inorganic molecules.[3,4] The oxidation chemistry is based on higher oxidation state hydroxo or oxo complexes which are obtained by oxidation and proton loss from aqua complexes of M^{II} (M = Ru, Os), e.g., eq 1 (bpy is 2,2′-bipyridine; py is pyridine).

$$cis\text{-}[Ru^{II}(bpy)_2(py)(H_2O)]^{2+} \xrightarrow{-e,\,-H^+} cis\text{-}[Ru^{III}(bpy)_2(py)(OH)]^{2+} \quad (1a)$$

$$cis\text{-}[Ru^{III}(bpy)_2(py)(OH)]^{2+} \xrightarrow{-e,\,H^+} cis\text{-}[Ru^{IV}(bpy)_2(py)(O)]^{2+} \quad (1b)$$

Thermodynamic studies have revealed that oxidation is coupled with proton loss because O → M^{III} or M^{IV} electronic donation leads to an enhanced acidity in the higher oxidation states.[3a,b,5]

A variety of mechanisms are available to the oxidized forms of these complexes, and the oxidative reactivity is extensive. It includes reactions with Cl^-,[3c,d,6] H_2O,[3e,f] H_2O_2,[7] sulfides,[8]

† This paper was presented in part at The Pittsburgh Conference, Atlanta, GA, March 7, 1989.

* Abstract published in *Advance ACS Abstracts*, September 15, 1993.

(1) Eberhard, S. In *Topics in Current Chemistry*; Springer-Verlag: New York, 1987; Vol. 142, p 1.

(2) (a) Murray, R. W. In *Electrochemical Chemistry*; Bard, A. J., Ed.; Marcel Dekker: New York, 1984; Vol. 13, p 191. (b) Anson, F. C.; Blauch, D. N.; Saveant, J. M.; Shu, C. F. *J. Am. Chem. Soc.* **1991**, *113*, 1922.

(3) (a) Takeuchi, K. J.; Thompson, M. S.; Pipes, D. W.; Meyer, T. J. *Inorg. Chem.* **1984**, *23*, 1845. (b) Takeuchi, K. J.; Samuels, G. J.; Gilbert, J. A.; Meyer, T. J. *Inorg. Chem.* **1983**, *22*, 1407. (c) Vining, W. J.; Meyer, T. J. *J. Electroanal. Chem. Interfacial Electrochem.* **1985**, *195*, 183. (d) Vining, W. J.; Meyer, T. J. *Inorg. Chem.* **1986**, *25*, 2015. (e) Gilbert, J. A.; Eggleston, D. S.; Murray, R. W.; Geselowitz, D. A.; Gersten, S. W.; Hodgson, D. J.; Meyer, T. J. *J. Am. Chem. Soc.* **1985**, *107*, 1985. (f) Gersten, S. W.; Samuels, G. J.; Meyer, T. J. *J. Am. Chem. Soc.* **1982**, *104*, 4029. (g) Moyer, B. A.; Thompson, M. S.; Meyer, T. J. *J. Am. Chem. Soc.* **1980**, *102*, 2310. (h) Dovletoglou, A.; Adeyemi, S. A.; Lynn, M. H.; Hodgson, D. J.; Meyer, T. J. *J. Am. Chem. Soc.* **1990**, *112*, 8989 and references therein. (i) Collin, J. P.; Sauvage, J. P. *Inorg. Chem.* **1986**, *25*, 135. (j) Bailey, C. L.; Drago, R. S. *Chem. Commun.* **1987**, 179. (k) Binstead, R. A.; Meyer, T. J. *J. Am. Chem. Soc.* **1987**, *109*, 3287. (l) Adeyemi, S. A.; Dovletoglou, A.; Guadalupe, A. R.; Meyer, T. J. *Inorg. Chem.* **1992**, *31*, 1375 and references therein. (m) Roecker, L.; Kutner, W.; Gilbert, J. A.; Simmons, M.; Murray, R. W.; Meyer, T. J. *Inorg. Chem.* **1985**, *24*, 3784. (n) Llobet, A.; Doppelt, P.; Meyer, T. J. *Inorg. Chem.* **1988**, *27*, 514. (o) Meyer, T. J. *J. Electrochem. Soc.* **1984**, *131*, 221C.

(4) (a) Che, C.-M.; Wing-Wah, Y. V. *J. Am. Chem. Soc.* **1987**, *109*, 1262. (b) Rotzinger, F. P.; Munavalli, S.; Comte, P.; Hurst, J. K.; Grätzel, M.; Pern, F. J.; Frank, A. J. *J. Am. Chem. Soc.* **1987**, *109*, 6619. (c) Wong, K. Y.; Che, C.-M.; Anson, F. C. *Inorg. Chem.* **1987**, *26*, 737. (d) Che, C.-M.; Wong, K. Y.; Anson, F. C. *J. Electroanal. Chem. Interfacial Electrochem.* **1987**, *226*, 737. (e) Maduro, J. M.; Chiericato, G.; De Giovani, W. F.; Romero, J. R. *Tetrahedron Lett.* **1988**, *29*, 765. (f) McHatton, R. C.; Anson, F. C. *Inorg. Chem.* **1984**, *23*, 3935. (g) Leung, W. H.; Che, C.-M. *J. Chem. Soc., Chem. Commun.* **1987**, 1376. (h) Wong, K. Y.; Anson, F. C. *J. Electroanal. Chem. Interfacial Electrochem.* **1987**, *237*, 69. (i) Leung, W. H.; Che, C.-M. *J. Am. Chem. Soc.* **1989**, *111*, 8812. (j) Che, C.-M.; Yam, V. W-W.; Mak, T. C. W. *J. Am. Chem. Soc.* **1990**, *112*, 2284.

(5) (a) Dobson, J. C. Ph.D. Thesis, The University of North Carolina at Chapel Hill, 1988. (b) Dobson, J. C.; Meyer, T. J. *Inorg. Chem.* **1988**, *27*, 3283.

(6) Ellis, C. D.; Gilbert, J. A.; Murphy, W. R.; Meyer, T. J. *J. Am. Chem. Soc.* **1983**, *105*, 4842.

0020-1669/93/1332-5502$04.00/0

Scheme I[a]

$$Ru^{VI}b_2(O)_2^{2+} \xrightarrow{+1.07} Ru^{V}b_2(O)(OH)^{2+} \xrightarrow{+0.94} Ru^{IV}b_2(O)(OH_2)^{2+} \xrightarrow{+0.76} Ru^{III}b_2(OH)(OH_2)^{2+} \xrightarrow{+0.50} Ru^{II}b_2(OH_2)_2^{2+}$$

(pH = 4, μ = 0.1, at 22 ± 2° vs. SSCE)

[a] b is 2,2′-bipyridine.

alcohols,[9] hydrocarbons,[10] olefins,[11a] and phenols.[11c] It has also been shown that oxo complexes of Ru^{IV} can act as homogeneous electrochemical catalysts[3g] and that the catalytic behavior is retained upon ion exchange into Nafion films.[3c,d]

In this paper we describe the preparation of thin polymeric films containing metal complexes in which the oxo–aqua chemistry is retained and electrocatalysis is observed. Two types of films were studied. Both were prepared by the electropolymerization of complexes that at the same time were aqua precursors and contained ligands having polymerizable functional groups. One type of film was prepared by coreductive electropolymerization[12] of $[Ru(vbpy)_2(CO_3)]$ in the presence of $[Ru(vbpy)_3]^{2+}$ (vbpy is

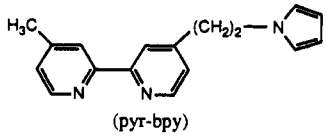

(pyr-bpy)

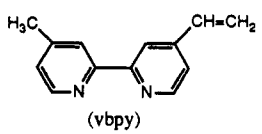

(vbpy)

4-methyl-4′-vinyl-2,2′-bipyridine). Subsequent addition of aqueous acid and proton-assisted aquation of carbonate anion gives a diaqua complex which is a precursor to high-oxidation-state oxo complexes.

The second type of film was prepared by oxidative electropolymerization[13] of $[Ru(pyr\text{-}bpy)_2(CO)_3]$ or $[Ru(pyr\text{-}bpy)_2Cl_2]$ (pyr-bpy is 4-(2-pyrrol-1-ylethyl)-4′-methyl-2,2′-bipyridine). The analogous diaqua complex was obtained by hydrolysis of the carbonato or chloro ligands.

The choice of the diaqua complex for incorporation into the film environment seemed especially appropriate. The redox chemistry of its solution analog, *cis*-$[Ru(bpy)_2(H_2O)_2]^{2+}$, had been investigated in some detail.[5] This complex undergoes stepwise oxidation to Ru^{VI} through the reversible couples $Ru^{III/II}$, $Ru^{IV/III}$, $Ru^{V/IV}$, and $Ru^{VI/V}$. The potentials for the various couples at pH = 4 are shown in the Latimer diagram in Scheme I.[5]

Although promising as a possible *cis*-directed, four-electron oxidant in solution, *cis*-$[Ru^{VI}(bpy)_2(O)_2]^{2+}$ is unstable with regard to loss of bpy and decomposition to give *trans,cis*-$[Ru^{VI}(bpy)(O)_2(OH)_2]$.[5] The driving force for this reaction comes from the electronic stabilization associated with the formation of the d^2 *trans*-dioxo group in the mono-bpy product.[3h-j,l]

While this paper was in preparation, a preliminary communication appeared describing the formation of poly-*cis*-$[Ru(pyr\text{-}bpy)_2Cl_2]$, its aquation, and the catalytic oxidation of benzyl alcohol to give benzaldehyde.[13i]

Experimental Section

Materials. Pyrrole was purified by vacuum distillation before use. The compound 4-methyl-4′-vinyl-2,2′-bipyridine (vbpy) was used as received from Du Pont. The salt tetra-*n*-butylammonium hexafluorophosphate, $[N(n\text{-}C_4H_9)_4](PF_6)$, was recrystallized from ethyl acetate in the presence of activated charcoal and further dried in a vacuum oven at room temperature for 2 days. Tetra-*n*-butylammonium perchlorate, $[N(n\text{-}C_4H_9)_4](ClO_4)$ (Aldrich), and lithium perchlorate (Alfa) were recrystallized before use. Acetonitrile (Burdick and Jackson) and methylene chloride (Fisher Scientific) were dried over 4-Å molecular sieves. The buffers were prepared from analytical reagent grade salts and acids. The following acids and salts were used at the indicated pH: $HClO_4$ or CF_3COOH (pH 1), $CF_3COOH/NaOH$ (pH 2), $CF_3COOH/Na[CH_3CO_2]$ (pH 3.6, 4.4), $NaH_2PO_4/NaOH$ (pH 5.9, 7.1, 7.9), $NaHCO_3/NaOH$ (pH 10.2), and $NaHPO_4/NaOH$ (pH 11.0, 11.9). Solvents and other reagents were of analytical reagent grade and were used as received. NanoPure water was used in all experiments involving aqueous solutions.

Measurements. Electrochemical measurements were performed with an EG&G PAR universal programmer, Model 175, coupled to a potentiostat–galvanostat, Model 173. A homemade coulometer was used for electrolysis. UV–vis spectra were recorded on an HP Model 8451A diode array spectrophotometer. Rotating disk electrode (RDE) experiments were performed with a Pine Instruments Co. rotator. Glassy carbon electrodes mounted on Teflon were used as working electrodes, and a coiled platinum wire was used as the auxiliary electrode. The surface area of the carbon electrode was 0.071 cm^2. Indium-doped tin oxide (ITO) optically transparent electrodes (Delta Technologies) were used for the spectroelectrochemical experiments. The reference for electrochemical measurements was the saturated sodium chloride calomel electrode (SSCE) without correction for junction potentials. Electrochemical cells were of common design. Platinum foil (0.254 cm^2) electrodes and $Si/SiO_2/Au$ electrodes[14] were used for IR measurements. Infrared spectra were recorded on a Nicolet 20DX FTIR spectrometer with a variable-angle specular reflectance attachment (Barnes Analytical).

Syntheses. (a) 4-(2-Pyrrol-1-yl-ethyl)-4′-methyl-2,2′-bipyridine (pyr-bpy). This compound was prepared by a slight modification of a previously published procedure.[15] A 1.0-mL volume of freshly distilled pyrrole and 8.1 mg of metallic sodium (cleaned in hexane and methanol) were deaerated with N_2, and the mixture was heated until all the sodium was dissolved. The resultant mixture was allowed to cool slightly above room temperature, and 503 mg of vbpy dissolved in a small amount of pyrrole was added by syringe. The mixture was heated at reflux for 2 h under N_2. Dry methanol (5 mL) was added, followed by ice water, and the resulting mixture was extracted with three 15-mL portions of ether. The organic layer was dried over Na_2SO_4. The solvent was removed by rotary evaporation, and the resulting oil was purified by using a silica column with ether as both solvent and eluant. A white solid was obtained by evaporating the solvent. It was characterized by ^1H-NMR (yield 50%).[15] The compound slowly polymerized in solution.

(b) $[Ru(vbpy)_3](PF_6)$. This salt was prepared according to a published procedure[12b] and was characterized by UV–visible, ^1H-NMR, and electrochemical measurements.

(c) *cis*-$[Ru(vbpy)_2Cl_2]\cdot 2H_2O$. To a 30-mL volume of 2:1 (v:v) 1,2-dimethoxyethane/MeOH previously deaerated with N_2 were added 66.9

(7) (a) Gilbert, J. A.; Roecker, L.; Meyer, T. J. *Inorg. Chem.* **1987**, *26*, 1126. (b) Gilbert, J. A.; Gersten, S. W.; Meyer, T. J. *J. Am. Chem. Soc.* **1982**, *104*, 6872.
(8) Roecker, L.; Dobson, J. C.; Vining, W. J.; Meyer, T. J. *Inorg. Chem.* **1987**, *26*, 779.
(9) (a) Roecker, L.; Meyer, T. J. *J. Am. Chem. Soc.* **1987**, *109*, 746. (b) Thompson, M. S.; Meyer, T. J. *J. Am. Chem. Soc.* **1982**, *104*, 4106.
(10) Thompson, M. S.; Meyer, T. J. *J. Am. Chem. Soc.* **1982**, *104*, 5070.
(11) (a) Seok, W. K.; Dobson, J. C.; Meyer, T. J. *Inorg. Chem.* **1988**, *27*, 3. (b) Seok, W. K.; Dobson, J. C.; Meyer, T. J. *Inorg. Chem.* **1986**, *25*, 1514. (c) Seok, W. K.; Meyer, T. J. *J. Am. Chem. Soc.* **1988**, *110*, 7358.
(12) (a) Ikeda, T.; Schmehl, R.; Denisevich, P.; William, K.; Murray, R. W. *J. Am. Chem. Soc.* **1982**, *104*, 2683. (b) Abruna, H. D.; Denisevich, P.; Umana, M.; Meyer, T. J.; Murray, R. W. *J. Am. Chem. Soc.* **1981**, *103*, 1. (c) Calvert, J. M.; Schmehl, R. H.; Sullivan, B. P.; Facci, J. S.; Meyer, T. J.; Murray, R. W. *Inorg. Chem.* **1983**, *22*, 2151.
(13) (a) Deronzier, A.; Essahalli, M.; Moutet, J. C. *J. Chem. Soc., Chem. Commun.* **1987**, 773. (b) Cosnier, S.; Deronzier, A.; Moutet, J. C. *J. Electroanal. Chem. Interfacial Electrochem.* **1983**, *207*, 315. (c) Deronzier, A.; Essahalli, M.; Moutet, J. C. *J. Electroanal. Chem. Interfacial Electrochem.* **1988**, *244*, 163. (d) Cosnier, S.; Deronzier, A.; Moutet, J. C. *J. Electroanal. Chem. Interfacial Electrochem.* **1985**, *193*, 193. (e) Eaves, J. G.; Munro, H. S.; Parker, D. *J. Chem. Soc., Chem. Commun.* **1985**, 684. (f) Bidan, G.; Deronzier, A.; Moutet, J. C. *Nouv. J. Chim.* **1984**, *8* (8-9), 398. (g) Eaves, J. G.; Munro, H. S.; Parker, D. *Inorg. Chem.* **1987**, *26*, 644. (h) Deronzier, A.; Moutet, J. C. *Acc. Chem. Res.* **1989**, *22*, 249 and references therein. (i) De Giovani, W. F.; Deronzier, A. *J. Chem. Soc., Chem. Commun.* **1992**, 1461.
(14) The $Si/SiO_2/Au$ layered electrodes were provided by the group of R. W. Murray at The University of North Carolina.
(15) Reich, H. E.; Levine, R. *J. Am. Chem. Soc.* **1955**, *77*, 4913.

mg of $RuCl_3 \cdot 3H_2O$ (0.26 mmol), 101.6 mg of vbpy (0.52 mmol), 70 mg of hydroquinone (H_2Q) (0.64 mmol), and 346.6 mg of LiCl (8 mmol). The mixture was heated at reflux for 3 h. The reaction was monitored by UV–visible spectroscopy. After 3 h, the mixture was cooled to room temperature and the solvent was removed by rotary evaporation. The resulting solid was dissolved in methylene chloride, the solution was filtered to remove LiCl, and extracted with cold water until the water layer became clear (usually three or four times with 20 mL of distilled water). The organic layer was separated from the mixture and dried over $MgSO_4$. The complex was precipitated by adding ether, collected by filtration, and dried overnight in a vacuum oven at room temperature (yield 78%, based on the dihydrate). Anal. Found (calcd): C, 52.10 (52.00); H, 4.31 (4.66); N, 9.34 (9.33); Cl, 14.34 (14.83).

(d) *cis*-[Ru(pyr-bpy)$_2$Cl$_2$]·2H$_2$O. A 30-mL volume of 2:1 (v:v) DME/MeOH was deaerated with N_2, and 50.2 mg (0.19 mmol) of $RuCl_3 \cdot 3H_2O$, 100.2 mg (0.38 mmol) pyr-bpy, 52.4 mg (0.48 mmol) of hydroquinone, and 326.5 mg (8 mmol) of LiCl were added. The mixture was heated at reflux overnight. The formation of the complex was verified by the appearance of its characteristic UV–visible spectrum. The mixture was purified by using a literature procedure[12a] (yield 74%, based on the dihydrate). Anal. Found (calcd): C, 56.01 (55.59); H, 4.89 (5.18); N, 11.18 (11.44); Cl, 10.13 (9.67).

(e) [Ru(pyr-bpy)$_2$(CO$_3$)]·2H$_2$O. A 50.3-mg quantity (0.069 mmol) of *cis*-$[Ru(pyr\text{-}bpy)_2Cl_2] \cdot 2H_2O$ was dissolved in 10 mL of MeOH, and 133.6 mg (1.0 mmol) of Na_2CO_3 was dissolved in 10 mL of H_2O. The solutions were mixed, deaerated with N_2, and heated at reflux for 3 h under N_2. The solvent was completely removed by rotary evaporation, and the residue was dissolved in methylene chloride and filtered to remove sodium carbonate. The organic layer was extracted with 25 mL of cold NaOH (pH 9), dried over $MgSO_4$, filtered to remove $MgSO_4$, and concentrated; the dark black solid was precipitated by adding ether. The solid was purified further by Soxhlet extraction with dry methylene chloride under N_2. The solution was concentrated, and the solid was precipitated by adding ether and then dried in vacuum at room temperature overnight (yield 83%, based on the dihydrate). Anal. Found (calcd): C, 57.55 (58.09); H, 5.29 (5.26); N, 11.24 (11.62); O, 9.02 (11.07).

(f) [Ru(vbpy)$_2$(CO$_3$)]·2H$_2$O. A 243.1-mg quantity (2 mmol) of Na_2CO_3 was dissolved in 10 mL of H_2O, and the solution was added to 10 mL of MeOH containing 109.2 mg (0.18) mmol) of *cis*-$[Ru(pyr\text{-}bpy)_2Cl_2] \cdot 2H_2O$. The procedures for the synthesis and purification steps were the same as for the pyr-bpy derivative described above (yield 78%, based on the dihydrate). Anal. Found (calcd): C, 52.16 (52.01); H, 4.77 (4.41); N, 8.66 (9.51); O, 13.69 (13.58).

Electropolymerization. (a) Polymeric films of poly-*cis*-[Ru(vbpy)$_2$(H$_2$O)$_2$](PF$_6$)$_2$-*co*-[Ru(vbpy)$_3$](PF$_6$)$_2$ were prepared on glassy carbon electrodes of surface area 0.071 cm^2 in a drybox by cycling from 0 to −1.5 V vs SSCE in acetonitrile 0.1 M in $[N(n\text{-}C_4H_9)_4](PF_6)$ containing varying ratios of $[Ru(vbpy)_3](PF_6)_2$ and $[Ru(vbpy)_2(CO_3)]$ with the total ruthenium concentration fixed at 5×10^{-4} M. A single-compartment cell with a three-electrode configuration was used in all experiments. The bis(aqua) complex was generated from the carbonato complex following electropolymerization by soaking the film-coated electrodes in water for 15 min and cycling through the $Ru^{III/II}$ couples in 0.1 M $HClO_4$.

(b) Films of poly-*cis*-[Ru(pyr-bpy)$_2$(H$_2$O)$_2$](ClO$_4$)$_2$ were prepared by oxidative electropolymerization of $[Ru(pyr\text{-}bpy)_2CO_3]$ in a drybox by holding the potential of a glassy carbon electrode (0.071 cm^2) at +1.3 V vs SSCE (usually for 15 min) in methylene chloride 3 mM in $[Ru(pyr\text{-}bpy)_2(CO_3)]$ and 0.1 M in tetra-*n*-butylammonium perchlorate. The bis(aqua) complex was generated as described above.

(c) Films of poly-*cis*-[Ru(pyr-bpy)$_2$Cl$_2$] were prepared by following the same procedure described above for the poly-$[Ru(pyr\text{-}bpy)_2(CO_3)]$ film but by using *cis*-$[Ru(pyr\text{-}bpy)_2Cl_2]$ in CH_2Cl_2 instead of the carbonato complex.

The surface coverages could be varied by controlling the number of scans or the time held at a fixed potential. Surface coverages (Γ in mol/cm^2) were determined by integrating the oxidative component of the $Ru^{III/II}$ wave in slow scan rate cyclic voltammograms (20 mV/s) in 0.1 M $HClO_4$ solutions. Surface coverages were typically in the range $\Gamma \sim 10^{-8}$–10^{-9} mol/cm^2.

Kinetic Measurements. Electrochemical oxidation of poly-*cis*-$[Ru^{II}(pyr\text{-}bpy)_2(H_2O)_2]^{2+}$ to the Ru^{III} complex was carried out on an ITO electrode in a three-component cell by holding the electrode at +0.7 V in $HClO_4$ (0.1 M). The spectral changes in the films were monitored spectrophotometrically. Absorbance–time traces were collected by using a diode array spectrophotometer and analyzed at 312 and 504 nm by assuming first-order kinetics (eq 2, where A_∞ and A_0 are the final and

$$\ln |A_\infty - A_t| = -k_{obs}t + \ln |A_\infty - A_0| \quad (2)$$

initial absorbances and A_t is the absorbance at time t). Data were collected over several half-lives, and first-order rate constants, k_{obs}, were calculated by using an unweighted least-squares fit.

Electrocatalytic Oxidations of Benzyl Alcohol and Chloride Ion. The electrocatalytic oxidations of benzyl alcohol and Cl^- at poly-*cis*-$[Ru(pyr\text{-}bpy)_2(H_2O)_2]^{2+}$ were studied by cyclic voltammetry and by rotating-disk voltammetry. The polymer was formed on glassy carbon electrodes as described above.

The oxidation of benzyl alcohol ($1\text{–}10^{-4}$ M) was studied in an acetate buffer at pH 4.5 with $NaClO_4$ at 0.5 M added to maintain constant ionic strength. Experiments were also conducted with the α,α'-deuterated alcohol $C_6H_5CD_2OH$ in order to determine the C–H/C–D kinetic isotope effect. Rotation rates were varied from 0 to 5000 rpm.

Kinetics of chloride oxidation were studied similarly. In the controlled-potential electrolysis experiments a glassy carbon electrode coated with poly-*cis*-$[Ru(pyr\text{-}bpy)_2(H_2O)_2]^{2+}$ was held at +1.4 V (vs SSCE) in 0.1 M HCl aqueous solution for ~2.0 h in a three-compartment cell. Chlorine analysis was performed by thiosulfate titration in water.

Results

Films of poly-*cis*-[Ru(pyr-bpy)$_2$Cl$_2$] and poly-[Ru(pyr-bpy)$_2$(CO$_3$)]. Polymeric films of poly-*cis*-$[Ru(pyr\text{-}bpy)_2Cl_2]$ and poly-$[Ru(pyr\text{-}bpy)_2(CO_3)]$ were prepared by oxidative electropolymerization by using a procedure related to those reported for pyrrole alone[16] and for pyrrole–bipyridine complexes of Ru^{II} and Fe^{II}.[13] Oxidation leads to a coupling based on the pyrrole rings with the release of protons.[13h] The reactions were carried out by cycling between 0 and +1.3 V or by holding the potential at +1.3 V vs SSCE, which gave faster polymerization rates. It is known that under these conditions the conductivity of polypyrrole is destroyed.[16]

When soaked in acidic aqueous solutions, films containing poly-$[Ru(pyr\text{-}bpy)_2(CO_3)]$ or copolymeric films containing both poly-$[Ru(vbpy)_3](PF_6)_2$ and poly-$[Ru(vpby)_2(CO_3)]$ provided a convenient route to poly-*cis*-$[Ru(pyr\text{-}bpy)_2(H_2O)_2]^{2+}$

$$\text{poly-}[Ru(pyr\text{-}bpy)_2(CO_3)] + 2H^+ + H_2O \rightarrow \text{poly-}cis\text{-}[Ru(pyr\text{-}bpy)_2(H_2O)_2]^{2+} + CO_2 \quad (3a)$$

or to poly-*cis*-$[Ru(vbpy)_2(H_2O)_2]^{2+}$ in the copolymeric films

$$^1/_3\text{poly-}[Ru(vbpy)_2(CO_3)]\text{-}co\text{-}^2/_3\text{poly-}[Ru(vbpy)_3]^{2+} + {}^2/_3H^+ + {}^1/_3H_2O \rightarrow {}^1/_3\text{poly-}cis\text{-}[Ru(vbpy)_2(H_2O)_2]^{2+}\text{-}co\text{-}{}^2/_3\text{poly-}[Ru(vbpy)_3]^{2+} + {}^1/_3CO_2 \quad (3b)$$

The spectral and electrochemical properties of *cis*-$[Ru(pyr\text{-}bpy)_2Cl_2]$, *cis*-$[Ru(pyr\text{-}bpy)_2(H_2O)_2]^{2+}$, and $[Ru(pyr\text{-}bpy)_2(CO_3)]$ in solution and in the films are compared in Table I and in Figures 1 and 2. The two-band pattern in the visible spectrum in Figure 1 arises from a series of $d\pi(Ru^{II}) \rightarrow \pi_1^*(bpy)$ metal to ligand charge-transfer (MLCT) transitions.[17,18] At higher energy, ligand-centered $\pi \rightarrow \pi^*(bpy)$ transitions appear in the UV. The same pattern of UV–visible absorption bands was observed in polymeric films as for the monomers in solution.

(16) (a) Diaz, A. F.; Kanagawa, K. K.; Logan, L. A. *J. Electroanal. Chem. Interfacial Electrochem.* **1982**, *133*, 233. (b) Diaz, A. F.; Castillo, J. I. *J. Chem. Soc., Chem. Commun.* **1980**, 397. (c) Feldman, B. J.; Burgmayer, P.; Murray, R. W. *J. Am. Chem. Soc.* **1985**, *107*, 872. (d) Nalwa, H. S.; Rabe, J. G.; Schmidt, W. F.; Dalton, L. R. *Makromol. Chem. Rapid Commun.* **1986**, *7*, 533.
(17) Meyer, T. J. *Pure Appl. Chem.* **1986**, *58*, 1193.
(18) Ferguson, J.; Herren, F.; Krausz, E. R.; Maeder, M.; Vrbancich, J. *Coord. Chem. Rev.* **1985**, *64*, 21.

Table I. Electrochemical and Near-UV–Visible Spectral Data Obtained in CH_2Cl_2 or on an In(III)-Doped SnO_2 (ITO) Electrode with CH_2Cl_2 in the External Solution ($\Gamma = 10^{-8}$–10^{-9} mol/cm^2)

complex	Ru^{II} λ_{max} (nm)	$Ru^{III/II}$ $E_{1/2}$ (V)[a]
cis-$[Ru(bpy)_2Cl_2]$	380, 553	0.31
cis-$[Ru(pyr\text{-}bpy)_2Cl_2]$	380, 560	0.24
poly-*cis*-$[Ru(pyr\text{-}bpy)_2Cl_2]$	366, 556	0.20, 0.75[b]
$[Ru(bpy)_2(CO_3)]$	391, 585	0.30
$[Ru(pyr\text{-}bpy)_2(CO_3)]$	384, 566	0.24
poly-$[Ru(pyr\text{-}bpy)_2(CO_3)]$	380, 560	0.22
cis-$[Ru(pyr\text{-}bpy)_2(H_2O)_2]^{2+}$	365, 492[c]	0.59[c]
poly-cis-$[Ru(pyr\text{-}bpy)_2(H_2O)_2]^{2+}$	366, 494[c]	0.69[c]

[a] $E_{1/2}$ values vs SSCE in 0.1 M $[N(n\text{-}C_4H_9)_4](PF_4)$ unless otherwise noted. A glassy carbon electrode was used to obtain $E_{1/2}$ values for the solution couples. [b] From a μ-oxo-bridged impurity; see text. [c] In 0.1 M $HClO_4$ solution.

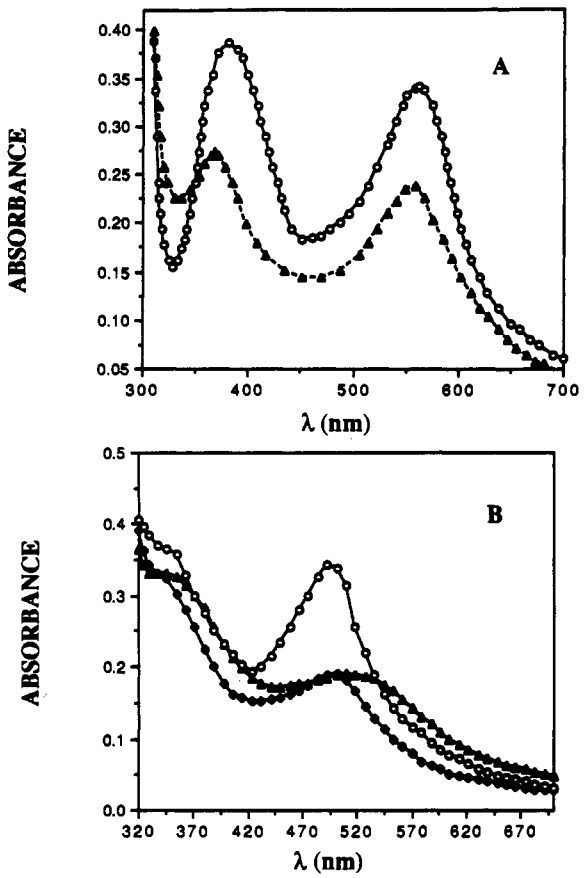

Figure 1. (A) UV–visible spectra of *cis*-$[Ru(pyr\text{-}bpy)_2Cl_2]$ in CH_2Cl_2 (2.1×10^{-5} M, 1-cm path length) (circles) and of poly-*cis*-$[Ru(pyr\text{-}bpy)_2Cl_2]$ on ITO with CH_2Cl_2 in the external solution (triangles). (B) UV–visible spectra of *cis*-$[Ru(pyr\text{-}bpy)_2(H_2O)_2]^{2+}$ (2×10^{-5} M) in $HClO_4$ at pH 1.0 (circles), poly-*cis*-$[Ru(pyr\text{-}bpy)_2(H_2O)_2]^{2+}$ on ITO with pH 1.0 HCl in the external solution (diamonds), and poly-*cis*-$[Ru(pyr\text{-}bpy)_2(H_2O)_2]^{2+}$ on ITO with a pH 10.2 $NaHCO_3/NaOH$ buffer in the external solution (triangles).

Shifts in λ_{max} between the solution phase and the film environment are expected, since the energies of MLCT bands are characteristically medium dependent.[17,18]

Representative cylic voltammograms are illustrated in Figure 2. As shown by the data in Table I, $E_{1/2}$ values for $Ru^{III/II}$ couples for the film and solution-based couples are comparable. For poly-*cis*-$[Ru(pyr\text{-}bpy)_2Cl_2]$ in $CH_2Cl_2/[N(n\text{-}C_4H_9)_4](PF_6)$ (0.1 M), the peak current (i_p) varies linearly with scan rate (v) in the range 10–100 mV/s as expected for a surface-confined electron transfer.[19] At $v \leq 20$ mV/s, the difference in the cathodic and anodic peak potentials (ΔE_p) was 40 mV ($\Gamma = 1.4 \times 10^{-9}$ mol/cm^2), which is consistent with slow electron transfer to the electrode.[2] Cyclic voltammograms obtained in methylene chloride that had not been scrupulously dried displayed an additional wave at +0.75 V due to the appearance of an oxo-bridged complex.[20]

The IR spectrum of a poly-$[Ru(pyr\text{-}bpy)_2(CO_3)]$ film deposited on a platinum foil electrode, displayed ν(C-H) stretching bands at 2800–3000 cm^{-1}, bpy ring stretching bands at 1725–1456 cm^{-1}, and a ClO_4^- band at 1100 cm^{-1}. Since the complex is neutral, the appearance of the ClO_4^- anions must be associated with oxidized pyrrole incorporated into the films as counterions during oxidative polymerization. For polypyrrole films, it is known that anionic migration into and out of the films accompanies oxidation and reduction.[21]

Substitution. (a) Solvolysis of poly-*cis*-$[Ru(pyr\text{-}bpy)_2Cl_2]$. When a glassy carbon electrode coated with poly-*cis*-$[Ru(pyr\text{-}bpy)_2Cl_2]$ was soaked in 0.1 M $HClO_4$ and cycled between 0 and +1.2 V (Figure 3B), the initial $Ru^{III/II}$ wave at $E_{1/2} = +0.24$ V was lost, with the concomitant appearance and subsequent disappearance of a wave at +0.42 V and with a final wave appearing at +0.59 V. The potentials and the stepwise nature of the changes are consistent with loss of Cl^- through an aqua–chloro intermediate.

$$\text{poly-}cis\text{-}[Ru(pyr\text{-}bpy)_2Cl_2] \xrightarrow{+H_2O,\,-Cl^-} \text{poly-}cis[Ru(pyr\text{-}bpy)_2(H_2O)Cl]^+ \quad (4a)$$

$$\text{poly-}cis\text{-}[Ru(pyr\text{-}bpy)_2(H_2O)Cl]^+ \xrightarrow{+H_2O,\,-Cl^-} \text{poly-}cis\text{-}[Ru(pyr\text{-}bpy)_2(H_2O)_2]^{2+} \quad (4b)$$

The aquation can be reversed by soaking the diaqua-containing film in saturated aqueous NaCl for 1 h, followed by drying the film under vacuum overnight. Anation did not occur simply by soaking the diaqua film in aqueous solution containing NaCl.

The aquation reaction was monitored spectrophotometrically by monitoring the growth and disappearance of poly-*cis*-$[Ru(pyr\text{-}bpy)_2(H_2O)Cl]^+$ at $\lambda_{max} = 520$ nm and the growth of poly-*cis*-$[Ru(pyr\text{-}bpy)_2(H_2O)_2]^{2+}$ at $\lambda_{max} = 494$ nm. From these measurements, the aquation of poly-*cis*-$[Ru(pyr\text{-}bpy)_2Cl_2]$ does not occur on a time scale of days by simple soaking. Rather, aquation at both stages was induced by cycling through the $Ru^{III/II}$ couple. After a scan, the aquation began to occur and continued to occur over a period of 2–4 h. The changes that occurred after a scan were monitored under conditions of no current flow by observing the changes in the rest potential of the electrode with time. After the rest potential stabilized, another scan led to further, time-dependent aquation. In later scans, as aquation neared completion, the rest potential took longer to reach equilibrium.

Attempts to electropolymerize *cis*-$[Ru(pyr\text{-}bpy)_2Cl_2]$ in $CH_3CN/0.1$ M $[N(n\text{-}C_4H_9)_4](PF_6)$ gave a film containing a mixture of the bis(chloro) and bis(acetonitrile) complexes ($E_{1/2}$ = +0.31 and +1.33 V).

(b) Solvolysis of poly-*cis*-$[Ru(pyr\text{-}bpy)_2(CO_3)]$. Previous work has shown that H^+-induced loss of CO_3^{2-} occurs from $Ru(bpy)_2(CO_3)$,[5] and the same chemistry was found in polymeric films. There is one unusual feature. Exposure to 0.1 M $HClO_4$ or HPF_6 causes CO_3^{2-} to be lost in sequential steps *via* the mono(aqua) mono(bicarbonato) complex as an intermediate; this can be inferred from the data in Figure 3A. There is no

(19) Bard, A. J.; Faulkner, L. R. *Electrochemical Methods: Fundamentals and Applications*; John Wiley & Sons: New York, 1980.

(20) (a) Chen, X.; Meyer, T. J. Unpublished results. (b) Geselowitz, D.; Meyer, T. J. *Inorg. Chem.* **1990**, *29*, 3894 and references therein.

(21) Kuwabata, S.; Yoneyama, H.; Tamura, H. *Bull. Chem. Soc. Jpn.* **1984**, *57*, 2247.

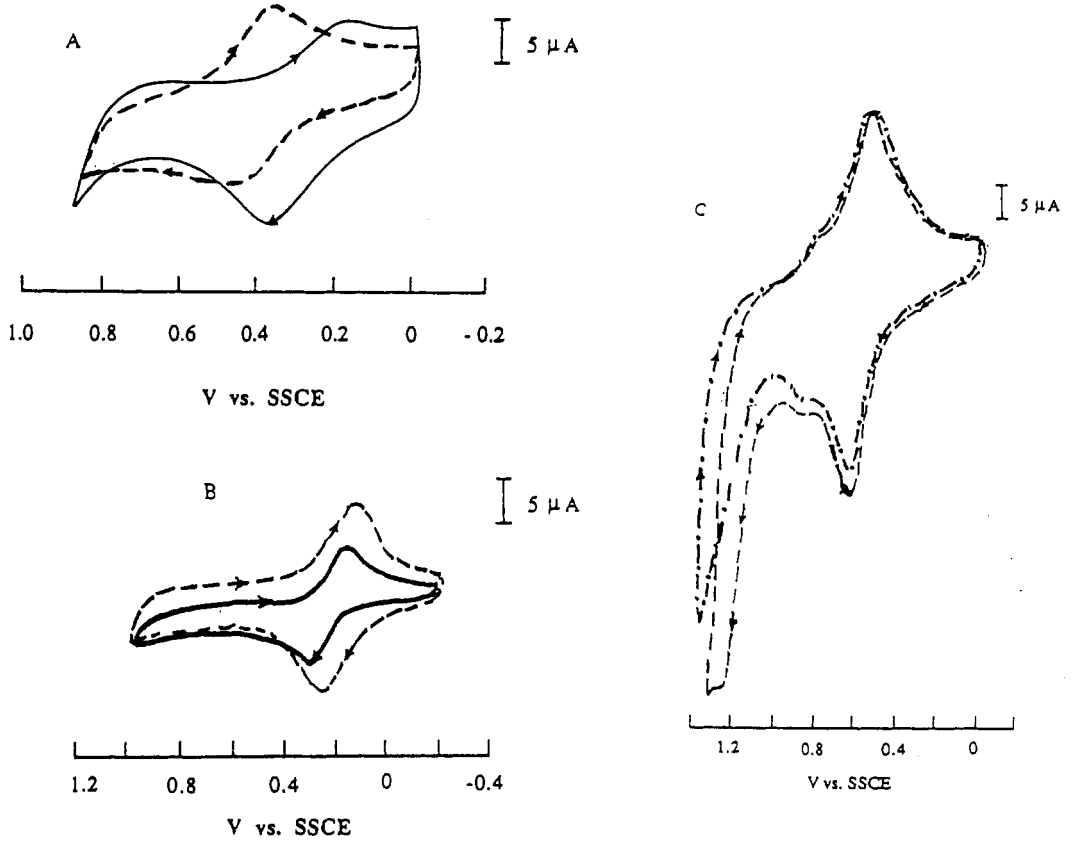

Figure 2. (A) Cyclic voltammograms of $Ru(pyr\text{-}bpy)_2(CO_3)$ (2.1×10^{-4} M) in $CH_2Cl_2/[N(C_4H_9)_4](PF_6)$ (0.1 M) at a glassy carbon electrode (0.071 cm^2) at a scan rate of 100 mV/s (dashed line) and of a poly-$[Ru(pyr\text{-}bpy)_2(CO_3)]$ film ($\Gamma = 2.2 \times 10^{-9}$ mol/cm^2) on a glassy carbon electrode (0.071 cm^2) with $CH_2Cl_2/[N(n\text{-}C_4H_9)_4](PF_6)$ (0.1 M) in the external solution (solid line) vs SSCE. (B) Cyclic voltammograms of *cis*-$Ru(pyr\text{-}bpy)_2Cl_2$ (1.0×10^{-4} M) in $CH_2Cl_2/[N(n\text{-}C_4H_9)_4](PF_6)$ (0.1 M) at a scan rate of 100 mV/s (solid line) and of poly-*cis*-$[Ru(pyr\text{-}bpy)_2Cl_2]$ with $CH_2Cl_2/[N(n\text{-}C_4H_9)_4](PF_6)$ (0.1 M) as the external solution on glassy carbon ($\Gamma = 1.4 \times 10^{-9}$ mol/cm^2) at a scan rate of 200 mV/s (dashed line). (C) Cyclic voltammogram of poly-*cis*-$[Ru(pyr\text{-}bpy)_2(H_2O)_2]^{2+}$ on glassy carbon ($\Gamma = 1.1 \times 10^{-8}$ mol/cm^2) in 0.1 M $HClO_4$ at a scan rate of 50 mV/s, showing the first (dashed line) and second scans (dashed and dotted line).

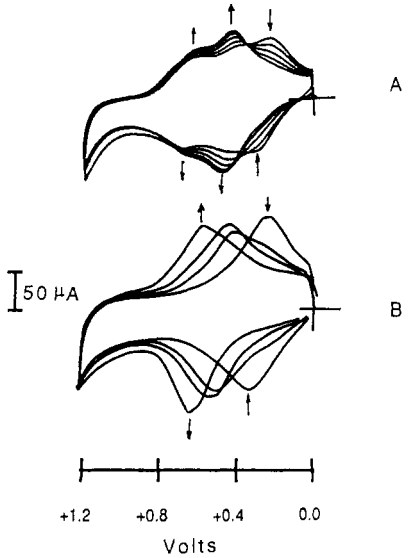

Figure 3. Successive scans at 50 mV/s on glassy carbon electrodes vs SSCE: (A) poly-$[Ru(pyr\text{-}bpy)_2(CO_3)]$ in 0.1 M HPF_6, $\Gamma = 1.0 \times 10^{-9}$ mol/cm^2; (B) poly-*cis*-$[Ru(pyr\text{-}bpy)_2Cl_2]$ in 0.1 M $HClO_4$, $\Gamma = 2.0 \times 10^{-9}$ mol/cm^2.

intermediate in the solution reaction.

$$\text{poly-}cis\text{-}[Ru(pyr\text{-}bpy)_2(CO_3)] \xrightarrow{H_3O^+} \text{poly-}cis\text{-}[Ru(pyr\text{-}bpy)_2(HCO_3)(H_2O)]^+ \quad (5a)$$

$$\text{poly-}cis\text{-}[Ru(pyr\text{-}bpy)_2(HCO_3)(H_2O)]^+ \xrightarrow{H_3O^+} \text{poly-}cis\text{-}[Ru(pyr\text{-}bpy)_2(H_2O)_2]^{2+} + CO_2 \quad (5b)$$

When a film of poly-*cis*-$[Ru(pyr\text{-}bpy)_2(CO_3)]$ was deposited in acetonitrile 0.1 M in $[N(n\text{-}C_4H_9)_4(ClO_4)]$ by cycling from 0 to +1.6 V, a reversible wave appeared at +0.22 V for the $Ru^{III/II}$ couple of poly-$[Ru(pyr\text{-}bpy)_2(CO_3)]$, and a quasi-reversible wave, at +1.33 V (ΔE_p = 80 mV, 50 mV/s) for the $Ru^{III/II}$ couple of poly-*cis*-$[Ru(pyr\text{-}bpy)_2(CH_3CN)_2]^{2+}$. After a few additional cycles, a new wave appeared at +0.76 V consistent with the $Ru^{III/II}$ couple for poly-*cis*-$[Ru(pyr\text{-}bpy)_2(HCO_3)(CH_3CN)]^+$. With continuous cycling, the wave at +0.22 V decreased in peak current, the wave at +1.33 V increased, and the peak current for the wave at +0.76 V remained constant. After 10 cyclings, the electrode was rinsed and transferred to an acetonitrile solution containing 0.1 M $[N(n\text{-}C_4H_9)_4](ClO_4)$. Only the waves at +0.76 and +1.33 V were observed. Under these conditions, $Ru(bpy)_2(CO_3)$ does not undergo solvolysis in CH_3CN, as shown by both electrochemical and UV–vis measurements.

When a film containing poly-*cis*-$[Ru(pyr\text{-}bpy)_2(CH_3CN)_2]^{2+}$ was cycled oxidatively in aqueous 0.1 M $HClO_4$ past the $Ru^{III/II}$ couple for the bis(acetonitrile) complex at +1.2 V, acetonitrile was lost during the first scan. The net reaction is shown in (6).

$$\text{poly-}cis\text{-}[Ru(pyr\text{-}bpy)_2(CH_3CN)_2]^{2+} + 2H_2O \rightarrow \text{poly-}cis\text{-}[Ru(pyr\text{-}bpy)_2(H_2O)_2]^{2+} + 2CH_3CN \quad (6)$$

The replacement of CH_3CN by H_2O was completed by cycling from 0 to +1.6 V three times. The acetonitrile complex could be recovered partially by repeated cycling in CH_3CN containing

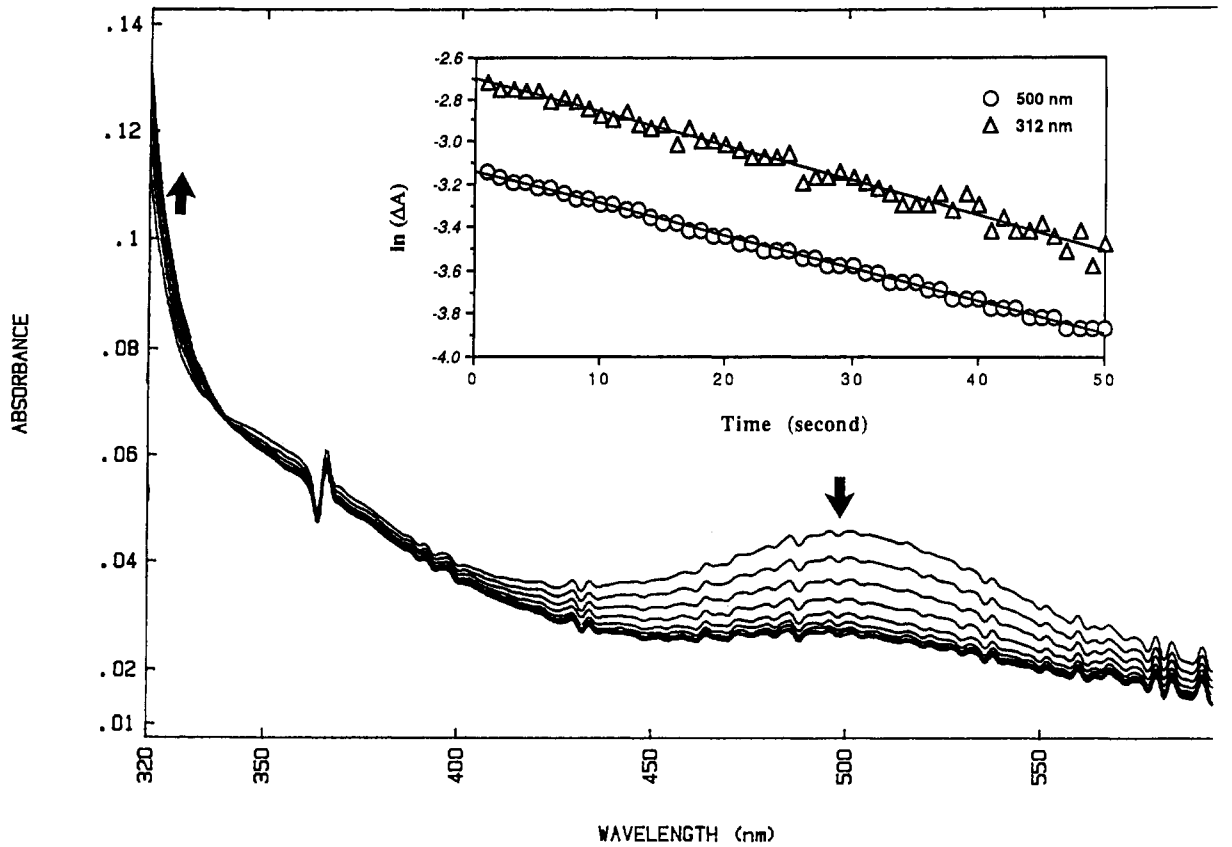

Figure 4. Oxidation of Ru(II) to Ru(III) in poly-*cis*-$[Ru(pyr\text{-}bpy)_2(H_2O)_2]^{2+}$ ($\Gamma = 1.8 \times 10^{-9}$ mol/cm^2) on ITO by potentiostating at +0.7 V vs SSCE with 0.1 M $HClO_4$ in the external solution. Shown are absorbance changes following a potential step to +0.7 V from $t = 0$ to $t = 34$ s, 1 s per scan. The first scan was obtained 2 s after the potential step. In the inset is shown a plot of ln ΔA vs time at 312 and 500 nm, where ΔA is the change in absorbance with time. The lines through the data are fits to the correlations $\ln |A_t - A_\infty|_{312nm} = \ln |A_0 - A_\infty|_{312nm} - kt$ with $k = 0.32$ s^{-1} ($R^2 = 0.98$) and $\ln |A_\infty - A_t|_{500nm} = \ln |A_\infty - A_0|_{500nm} - kt$ with $k = 0.65$ s^{-1} ($R^2 = 0.99$).

0.1 M $[N(n\text{-}C_4H_9)_4](ClO_4)$, as shown by the reappearance of the wave at $E_{1/2} = +1.33$ V.

Redox Properties of poly-*cis*-$[Ru(pyr\text{-}bpy)_2(H_2O)_2]^{2+}$. In Figure 2C are shown the first and second cyclic voltammograms of a poly-*cis*-$[Ru(pyr\text{-}bpy)_2(H_2O)_2]^{2+}$ film on a glassy carbon electrode immersed in aqueous 0.1 M $HClO_4$. The well-defined wave at +0.59 V and shoulder at +0.83 V appear at potentials that are near those for the $Ru^{III/II}$ and $Ru^{IV/III}$ couples of *cis*-$[Ru(bpy)_2(H_2O)_2]^{2+}$ at the same pH.[5] In solution at pH 1.0, additional waves appear for *cis*-$[Ru(bpy)_2(H_2O)_2]^{2+}$ at +1.10 ($Ru^{V/IV}$) and +1.26 V ($Ru^{VI/V}$). Well-defined waves for the higher oxidation state couples do not appear for the films. For freshly prepared films electropolymerized at +1.3 V, an irreversible oxidative wave appeared at +1.26 V but only on the first scan. Following the first scan, it was replaced by an irreversible oxidation wave with an onset at +1.3 V. Oxidation of polypyrrole films based on *N*-alkyl- and *N*-aryl-substituted pyrroles is known to occur at considerably lower potentials (–0.01 to +0.65 V vs SSCE), which argues against this wave being due to oxidation of the polymeric backbone.[16]

Oxidation of poly-*cis*-$[Ru(pyr\text{-}bpy)_2(H_2O)_2]^{2+}$ to Ru^{III} was sufficiently slow in the films that the reaction could be monitored by diode array spectrophotometry. The experiments were conducted by stepping the potential of a film-coated ITO optically transparent electrode from 0 to +0.7 V (vs SSCE) and following the changes in absorbance that occurred as a function of time in aqueous 0.1 M $HClO_4$ (Figure 4). Subsequent kinetic runs were conducted by reducing Ru^{III} back to Ru^{II} at 0.0 V, and another +0.7-V potential step was applied. At this potential, oxidation of Ru^{II} to Ru^{III} occurs for *cis*-$[Ru(bpy)_2(H_2O)_2]^{2+}$ at pH 1.[5] The oxidation of Ru^{II} was demonstrated by the decrease in absorbance of the MLCT band at 500 nm, and the appearance of Ru^{III}, by an increase at 310 nm. At the end of a kinetic run, there was evidence for some residual Ru^{II} (<30%). An isosbestic point was maintained at 341 nm. The absorbance changes with time followed first-order kinetics (Figure 4) with k_{obs}(310 nm) = 0.32 s^{-1} and k_{obs}(500 nm) = 0.65 s^{-1}. The difference in rate constants for the data at 310 and 500 nm for the first run are, at least in part, a consequence of the large experimental error.

There was a significant aging effect on k_{obs}. The measured rate constant for oxidation decreased by a factor of 4 in a second run and then to 0.016 s^{-1} on the third and successive runs.

The $Ru^{III/II}$ couple has the characteristics of a chemically reversible couple on glassy carbon, and there appeared to be no significant changes in ΔE_p for successive scans at scan rates as low as 10 mV/s. A plot of peak current (i_p) versus sweep rate was linear over the range 10–200 mV/s (surface coverage $\Gamma = 1.1 \times 10^{-8}$ mol/cm^2). The peak to peak potential separation was $\Delta E_p = 50$ mV at a scan rate of 50 mV/s.

The peak currents for the $Ru^{IV/III}$ couple were only a fraction of those for the $Ru^{III/II}$ couple. The same observation has been made for related solution couples where the diminished current has been attributed to kinetic effects.[3k]

Both couples were pH dependent on glassy carbon. Plots showing the variation in $E_{1/2}$ with pH for the two couples are shown in Figure 5, where, for comparison, plots for *cis*-$[Ru(bpy)_2(H_2O)_2]^{2+}$ are shown as dashed lines.[5] The $E_{1/2}$–pH regions where each of the oxidation states Ru^{II}, Ru^{III}, Ru^{IV} are dominant are labeled on the diagram. In certain pH regions, oxidation leads to a change in proton content between oxidation states and to a pH dependence of the couples. For example, from pH ~2 to pH ~5.2, the pH dependence is consistent with the couple in (7a).

From the data, additional pH-dependent regions can be inferred for the $Ru^{III/II}$ couple

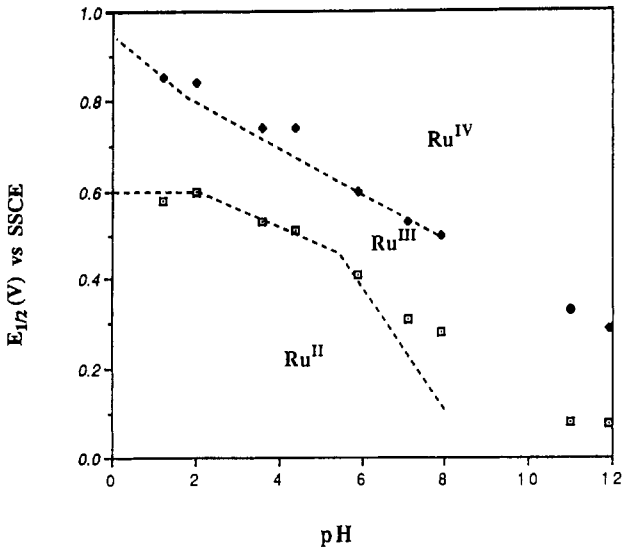

Figure 5. Plots of $E_{1/2}$ vs pH for the $Ru^{IV/III}$ and $Ru^{III/II}$ couples of poly-*cis*-$[Ru(pyr\text{-}bpy)_2(H_2O)_2]^{2+}$ on a glassy carbon electrode (μ = 0.1 M). The dashed lines show the pH dependence for the corresponding couples of *cis*-$[Ru(bpy)_2(H_2O)_2]^{2+}$ under the same conditions taken from ref 5.

poly-*cis*-$[Ru^{III}(pyr\text{-}bpy)_2(H_2O)(OH)]^{2+} + e + H^+ \rightarrow$
poly-*cis*-$[Ru^{II}(pyr\text{-}bpy)_2(H_2O)_2]^{2+}$ (7a)

poly-*cis*-$[Ru^{III}(pyr\text{-}bpy)_2(H_2O)_2]^{3+} + e \rightarrow$
poly-*cis*-$[Ru^{II}(pyr\text{-}bpy)_2(H_2O)_2]^{2+}$ (pH 0 to ~2) (7b)

poly-*cis*-$[Ru^{III}(pyr\text{-}bpy)_2(OH)_2]^{+} + e + 2H^+ \rightarrow$
poly-*cis*-$[Ru^{II}(pyr\text{-}bpy)_2(H_2O)_2]^{2+}$ (pH ~5 to ~11) (7c)

poly-*cis*-$[Ru^{III}(pyr\text{-}bpy)_2(OH)_2]^{+} + e + H^+ \rightarrow$
poly-*cis*-$[Ru^{II}(pyr\text{-}bpy)_2(OH)(H_2O)]^{+}$ (pH > ~11) (7d)

and for $Ru^{IV/III}$

poly-*cis*-$[Ru^{IV}(pyr\text{-}bpy)_2(O)(H_2O)]^{2+} + e + 2H^+ \rightarrow$
poly-*cis*-$[Ru^{III}(pyr\text{-}bpy)_2(H_2O)_2]^{3+}$ (pH <~2) (7e)

It is possible to estimate pK_a values from the breaks in the plots of $E_{1/2}$ vs pH in Figure 5.[5] Those estimates with corresponding values for the solution couples in parentheses are as follows: poly-*cis*-$[Ru^{III}(pyr\text{-}bpy)_2(H_2O)_2]^{3+}$, p$K_{a1}$ = 2.0 (1.5), pK_{a2} = 5–6 (5.2); *cis*-$[Ru^{II}(pyr\text{-}bpy)_2(H_2O)_2]^{2+}$, p$K_{a1}$ = ~7(?) (8.9), pK_{a2} > 11.0 (11.0).

The acid–base properties of the complexes are also apparent in UV–visible spectra. In Figure 1B are shown spectra of poly-*cis*-$[Ru(pyr\text{-}bpy)_2(H_2O)_2]^{2+}$ on ITO potentiostated at 0 V in pH 1 and pH 10 aqueous solutions. Above pH 8, the spectrum is red-shifted (from λ_{max} = 494 nm to λ_{max} = 510 nm). For *cis*-$[Ru(bpy)_2(H_2O)_2]^{2+}$ in water, an analogous spectral shift occurs with formation of the hydroxo complex, *cis*-$[Ru(bpy)_2(OH)(H_2O)]^{+}$,[5] and presumably, the same equilibrium exists within the films. The shift to lower energy for the MLCT bands arises because the OH^- ligand destabilizes the filled $(d\pi)^6$, levels decreasing the $d\pi \rightarrow \pi^*$(bpy) energy gap.

A spectroelectrochemical experiment was conducted in which a polymeric film of poly-*cis*-$[Ru(pyr\text{-}bpy)_2(H_2O)_2]^{2+}$ on ITO was potentiostated at different potentials in 0.1 M trifluoroacetic acid. The spectrum obtained at 0 V was that expected for Ru^{II} with λ_{max} = 492 nm (Figure 4). At 0.60 V, partial oxidation of Ru(II) to Ru(III) had occurred, as shown by the decrease in intensities of the $d\pi \rightarrow \pi_1^*$ and $d\pi \rightarrow \pi_2^*$ MLCT bands at 492 and 392 nm. Further oxidation at potentials above +1.0 V led to complete or nearly complete loss of the MLCT bands, consistent with oxidation of Ru(II). The spectral changes were reversible and occurred with an isosbestic point at 341 nm. When the potential of the electrode was returned to 0.0 V, the absorptions for Ru(II) were recovered quantitatively. The spectral changes occurred on a time scale of tens of seconds; recall the results of the kinetic study described above. From the slope and intercept of a plot of applied potential (E_{appl}) vs log([Ru^{III}]/[Ru^{II}]) (eq 8),

$$E_{appl} = E^{\circ\prime}(Ru^{III/II}) + \frac{0.059}{n}\log\frac{[Ru^{III}]}{[Ru^{II}]} \qquad (8)$$

the values $E^{\circ\prime}$ = 0.58 V ($E_{1/2}$ = 0.60 V from cyclic voltammetry) and n = 0.36 were obtained.[22] There is precedence for the deviation of the experimental value for n = 0.36 from the theoretical value of n = 1. It may reflect partial oxidation in the film.[22a]

Peak currents for the $Ru^{IV/III}$ and $Ru^{III/II}$ couples were dependent on pH and, somewhat, on the anion in the buffer. Data demonstrating the pH effect are shown in Table II as the ratio of peak current in the buffer to that in 0.1 M $HClO_4$ for the $Ru^{III/II}$ couple. These effects are reversible. When the electrolyte in the external solution was changed between buffers, the electrochemical responses became those appropriate to the new medium.

Table II. Effects of pH on Peak Currents for the $Ru^{III/II}$ Couple in Poly-*cis*-$[Ru(pyr\text{-}bpy)_2(H_2O)_2]^{2+}$ at μ = 0.1 Relative to 0.1 M $HClO_4$[a]

buffer	pH	$i_{p,a}/i_{p,a}$ (in 0.1 M $HClO_4$)
$Na(CF_3CO_2)/CF_3CO_2H$	1.2	0.78
	2.0	0.88
	4.4	0.58
$Na(CH_3CO_2)/CH_3CO_2H$	3.7	0.42
NaH_2PO_4/Na_2HPO_4	5.9	0.19
	7.1	0.14
	7.9	0.11
$NaHCO_3/Na_2CO_3$	10.2	0
Na_2HPO_4/Na_3PO_4	11.9	0.15

[a] The surface coverage was $\Gamma = 1.1 \times 10^{-8}$ mol/cm^2, on a glassy carbon electrode.

Oxidation of $^1/_3$poly-*cis*-$[Ru(vbpy)_2(H_2O)_2]^{2+}$-*co*-$^2/_3$poly-$[Ru(vbpy)_3]^{2+}$. Attempts to electropolymerize $[Ru(vbpy)_2(CO_3)]$ directly were unsuccessful. At the very negative potentials required (–2.0 V), complications arose from competing decomposition pathways. It was possible to prepare films with a content ~$^1/_3$ in poly-$[Ru(vbpy)_2(CO_3)]$ by copolymerization with $[Ru(vbpy)_3]^{2+}$ by holding the electrode potential at –1.5 V, which is past the first vbpy-based reduction wave for $[Ru(vbpy)_3]^{2+}$ but considerably more positive than the potential for the reduction of $[Ru(vbpy)_2(CO_3)]$.

A study was made of the compositions of films prepared from solutions containing $[Ru(vbpy)_2(CO_3)]$ and $[Ru(vbpy)_3]^{2+}$ relative to the solutions from which they were prepared. For these measurements, the carbonato complex was converted into the bis(aqua) complex by soaking in 0.1 M $HClO_4$ and cycling through

(22) (a) Cunningham, D. D.; Galal, A.; Pham, C. V.; Lewis, E. T.; Burkhardt, A.; Laguren-Davidson, L.; Nkansah, A.; Ataman, O. Y.; Zimmer, H.; Mark, H. B. *J. Electrochem. Soc., Electrochem. Sci. Technol.* **1988**, 2750. (b) DeAngelis, T. P.; Heineman, W. R. *J. Chem. Educ.* **1976**, *53*, 594.
(23) (a) Sosnoff, C. S. M.S. Thesis, The University of North Carolina at Chapel Hill, 1990. (b) Young, R. C.; Keene, F. R.; Meyer, T. J. *J. Am. Chem. Soc.* **1977**, *99*, 2648. (c) Chan, M.-S.; Wahl, A. C. *J. Phys. Chem.* **1978**, *82*, 2542. (d) Gardner, J.; Chen, X.; Meyer, T. J. Unpublished results.
(24) Gould, S. Ph.D. Thesis, The University of North Carolina at Chapel Hill, 1991, and references therein.
(25) Murray, R. W. *Annu. Rev. Mater. Sci.* **1984**, *14*, 145.

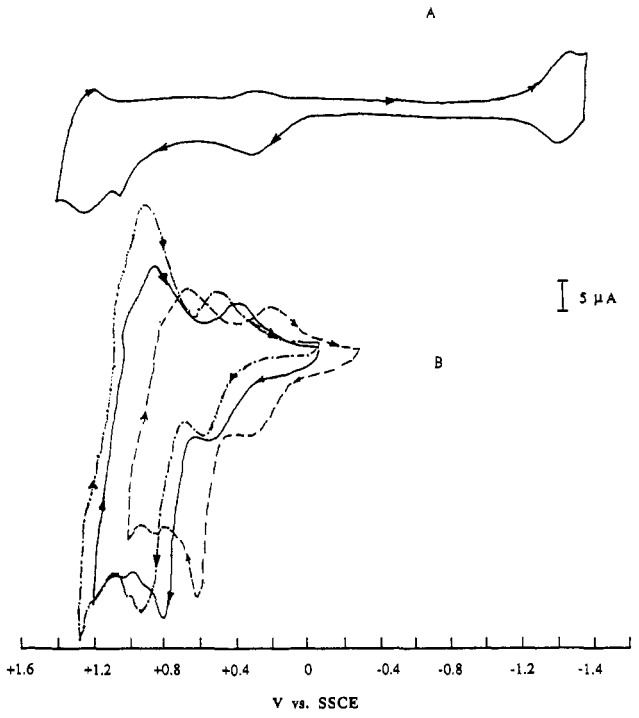

Figure 6. Cyclic voltammograms (vs SSCE) of (A) $^1/_3$poly-[Ru(vbpy)$_2$-(CO$_3$)-*co*-$^2/_3$poly-[Ru(vbpy)$_3$(PF$_6$)$_2$] in CH$_3$CN/[N(*n*-C$_4$H$_9$)$_4$](PF$_6$) (0.1 M) on glassy carbon at 50 mV/s and (B) $^1/_3$poly-[*cis*-Ru(vbpy)$_2$-(H$_2$O)$_2$]$^{2+}$-*co*-$^2/_3$poly-[Ru(vbpy)$_3$(PF$_6$)$_2$] on glassy carbon at 50 mV/s and pH 1.0 (HClO$_4$) (dashed and dotted line), pH 5.0 (NaOH/NaH$_2$PO$_4$) (solid line), and pH 8.7 (NaOH/Na$_2$HPO$_4$) (dashed line).

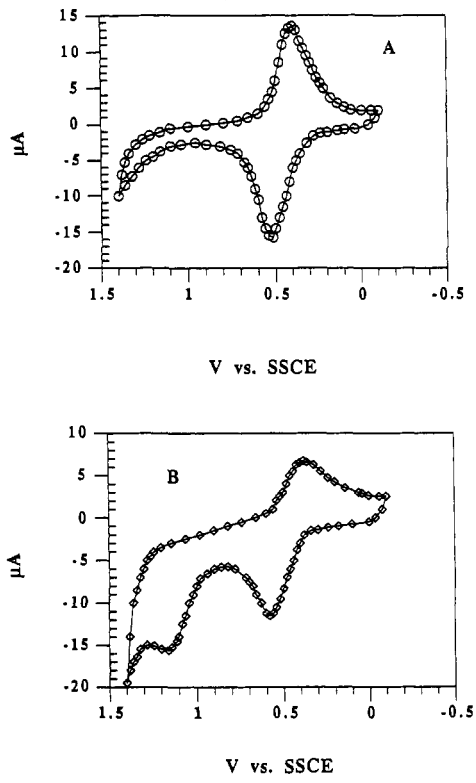

Figure 7. Cyclic voltammograms of poly-*cis*-[Ru(pyr-bpy)$_2$(H$_2$O)^2]$^{2+}$ on glassy carbon vs SSCE at 50 mV/s in pH 4.5 acetate buffer 0.5 M in NaClO$_4$: (A) [C$_6$H$_5$CD$_2$OH] = 1.9 M; (B) [C$_6$H$_5$CH$_2$OH] = 1.9 M.

the Ru$^{III/II}$ couple. The film compositions were estimated from the ratios of the Ru$^{III/II}$ waves for the two couples. The results as—solution composition (film composition)—were as follows: 90:10 (38:62), 75:25 (34:66), 70:30 (39:61), 50:50 (32:68).

A single-scan cyclic voltammogram of $^1/_3$poly-[Ru(vbpy)$_2$-(CO$_3$)-*co*-$^2/_3$poly-[Ru(vbpy)$_3$](PF$_6$)$_2$] in CH$_3$CN 0.1 M in [N(*n*-C$_4$H$_9$)$_4$](PF$_6$) is shown in Figure 6A. As for the polypyrrole-based film, a complication exists for the Ru$^{III/II}$ couple of the carbonato complex ($E_{p,a}$ = +0.34 V, $E_{p,c}$ = +0.30 V). Following an oxidative scan, the peak current for the return, reductive wave was smaller than that for the oxidative scan except at fast scan rates (>500 mV/s). Presumably, as in the polypyrrole film, oxidatively induced loss of the carbonato group occurs to give the bis(acetonitrile) complex whose Ru$^{III/II}$ couple overlaps with that of the poly-[Ru(vbpy)$_3$]$^{3+/2+}$ couple.

The carbonato complex was converted into the bis(aqua) complex in the film by soaking and cycling the modified electrode in 0.1 M HClO$_4$; a cyclic voltammogram of the resulting film is shown in Figure 6B. The initial scan provides evidence for the Ru$^{III/II}$ couples of poly-*cis*-[Ru(vbpy)$_2$(H$_2$O)$_2$]$^{3+/2+}$ ($E_{1/2}$ = +0.60 V) and poly-[Ru(vbpy)$_3$]$^{2+}$ ($E_{1/2}$ = +0.94 V) with additional oxidative waves appearing at E_p = +0.87, +0.98, and +1.10 V. When the film was soaked in a pH 5 buffer, the Ru$^{III/II}$ wave for the bis(aqua) couple appeared at $E_{1/2}$ = 0.51 V, a multielectron oxidation wave appeared at E_p = 0.89 V, and the Ru$^{III/II}$ wave for poly-[Ru(vbpy)$_3$$^{2+}$ remained at $E_{1/2}$ = 0.94 V. The pattern and potentials of the waves at pH 1 were similar to those for *cis*-[Ru(bpy)$_2$(H$_2$O)$_2$]$^{2+}$.[5] For this complex at pH 5, the Ru$^{III/II}$, Ru$^{IV/III}$, Ru$^{V/IV}$, and Ru$^{VI/V}$ couples are observed at $E_{1/2}$ = +0.45, +0.67, +0.90, and +1.04 V. After the first scan, the peak heights for the oxidative components of the waves involving oxidation states past Ru^{III} diminished, with clear evidence remaining for only the Ru$^{VI/V}$ couple. The loss of peak current after the first scan is permanent. The poly-[Ru(vbpy)$_3$]$^{3+/2+}$ couple was pH independent over the pH range 1–8.

Oxidation of Benzyl Alcohol and Chloride Ion. The electrocatalytic oxidation of benzyl alcohol (C$_6$H$_5$CH$_2$OH) at a poly-*cis*-[Ru(pyr-bpy)$_2$(H$_2$O)$_2$]$^{2+}$-coated glassy carbon electrode was investigated at pH 4.5 in a HOAc/NaOAc buffer with NaClO$_4$ (0.5 M) added to maintain constant ionic strength. Shown in Figure 7 are cyclic voltammograms in this medium with added benzyl alcohol and the α,α'-deuterated alcohol. In the voltammogram with added benzyl alcohol, a new wave appears at $E_{p,a}$ ~ 1.15 V. It appears to be triggered by the most positive couple in the first scan cyclic voltammogram in Figure 2C at +1.26 V. The current for this wave increased with added benzyl alcohol. Under these conditions, the background currents at a bare glassy carbon electrode or at a glassy carbon electrode coated with polypyrrole (Γ = 10^{-8} mol/cm^2) were much smaller (<10%).

Kinetic studies were conducted on a film having $\Gamma = 2.6 \times 10^{-8}$ mol/cm^2 by rotating-disk voltammetry. The current was monitored for potential sweeps from –0.1 V to +1.3 V as a function of added C$_6$H$_5$CH$_2$OH (10^{-4}–1 M) and rotation rate (0–5000 rpm). Within experimental error, there was no obvious dependence of the catalytic current (defined as the plateau current with and without added benzyl alcohol) on rotation rate within the concentration range, 0.38 mM ≤ [C$_6$H$_5$CH$_2$OH] ≤ 190 mM, as shown in Figure 8A.

In analyzing the voltammetric data, the mechanism shown in eqs 9–12 was assumed. In these equations C$_6$H$_5$CH$_2$OH$_f$ represents benzyl alcohol in the film and Ru^{IV} the Ru^{IV} sites in

$$C_6H_5CH_2OH \overset{K_p}{\rightleftarrows} C_6H_5CH_2OH_f \quad (9)$$

$$C_6H_5CH_2OH_f + Ru^{VI} \overset{K_A}{\rightleftarrows} C_6H_5CH_2OH_f, Ru^{VI} \quad (10)$$

$$C_6H_5CH_2OH_f, Ru^{VI} \overset{k}{\rightarrow} C_6H_5CH_2CHO + Ru^{IV} \quad (11)$$

$$Ru^{IV} \overset{k'}{\rightarrow} Ru^{VI} \quad (12)$$

the films that are active toward oxidation to Ru^{VI}. The quantities

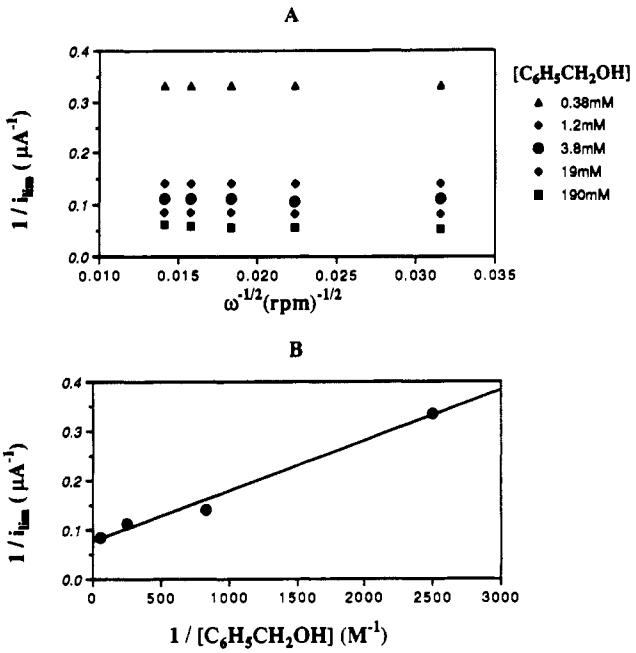

Figure 8. (A) Plots of i_{lim}^{-1} vs $\omega^{-1/2}$ from rotating-disk voltammograms (vs SSCE) on a film of poly-*cis*-$[Ru(pyr\text{-}bpy)_2(H_2O)_2]^{2+}$ ($\Gamma = 2.6 \times 10^{-8}$ mol/cm^2) (0.071 cm^2), at pH 4.5 in a HOAc/NaOAc buffer, $\mu = 0.5$ M $NaClO_4$, at various concentrations of $C_6H_5CH_2OH$. (B) Plot of i_{lim}^{-1} vs $[C_6H_5CH_2OH]^{-1}$. The linear correlation is to the equation $i_{lim}^{-1} = 7.5 \times 10^{-2} + 1.0 \times 10^{-4}[C_6H_5CH_2OH]^{-1}$ ($R^2 = 0.99$).

k and k' are rate constants for oxidation of benzyl alcohol by Ru^{VI} and reoxidation of Ru^{IV} to Ru^{VI}. The constant K_p is the equilibrium constant for partitioning the alcohol into the film, and K_A is the formation constant for the association complex between the alcohol and Ru^{VI} within the film.

On the basis of this mechanism, the reciprocal of the limiting current is predicted to vary with $[C_6H_5CH_2OH]$ as shown in eq 13 if the following assumptions are made: (1) The redox cycle

$$\frac{1}{i_{lim}} = (nFA\Gamma)^{-1}\left(\frac{1}{kK_AK_p[C_6H_5CH_2OH]} + \frac{1}{k}\right) \quad (13)$$

involves the $Ru^{VI/IV}$ couple and the electrochemical stoichiometry, $n = 2$. (2) The oxidized organic product is benzaldehyde (as it is in the oxidation of $C_6H_5CH_2OH$ by *cis*-$[Ru(bpy)_2(py)(O)]^{2+}$ and as shown in ref 13i).[9a] (3) The rate-limiting characteristics of the electrode are dictated by the oxidation of benzyl alcohol and not by reoxidation of Ru^{IV} to Ru^{VI}. (This is inferred from the $C_6H_5CH_2OH/C_6H_5CD_2OH$ kinetic isotope effect; vide infra.) (4) The concentration of $C_6H_5CH_2OH$ in the film is sufficiently high that its oxidation is kinetically pseudo first order in $[C_6H_5CH_2OH]$. (5) Diffusion to or into the films is facile and not rate limiting. (6) The catalytic current (i_{cat}) is far greater than the background current, so that the approximation $i_{lim} \approx i_{cat}$ holds. (7) The redox step can be partitioned into a preassociation equilibrium, characterized by an equilibrium constant K_A, and the redox step, k.

In eq 13, F is Faraday's constant, A the electrode surface area (cm^2), n the number of equivalents transferred ($n = 2$), and Γ the surface coverage ($\Gamma = 2.6 \times 10^{-8}$ mol/cm^2). Shown in Figure 8B is a plot of i_{lim}^{-1} vs $[C_6H_5CH_2OH]^{-1}$. From the intercept of the plot in Figure 8B and the known electrode surface area (0.071 cm^2), $K_AK_P = 798$ M^{-1} and $k = 0.37$ s^{-1}. From kinetic studies in aqueous solution with *cis*-$[Ru(bpy)_2(py)(O)]^{2+}$ as oxidant, it has been established that the oxidation of benzyl alcohol proceeds with a kinetic isotope effect, $C_6H_5CH_2OH/C_6H_5CD_2OH$, of 50 at 25 °C.[9a] Comparative peak current measurements for the oxidation of $C_6H_5CH_2OH$ or $C_6H_5CD_2OD$ at poly-*cis*-$[Ru(pyr\text{-}bpy)_2(H_2O)_2]^{2+}$ give $i_p(H)/i_p(D) \geq 29$ (Figure 7).

A preliminary study was also made of the oxidation of Cl^- by poly-*cis*-$[Ru(pyr\text{-}bpy)_2(H_2O)_2]^{2+}$ on glassy carbon. In cyclic voltammograms at a scan rate of 20 mV/s in the presence of added Cl^- (up to 1 M), an oxidative catalytic wave appeared at $E_p \sim 1.5$ V. The peak current for the catalytic wave increased with $[Cl^-]$ and was dependent on added counterions, with i_p decreasing in the order 0.1 M CF_3CO_2H > 0.1 M HCl > 0.1 M $HClO_4$, all with 0.1 M added NaCl.

Controlled-potential electrolysis in 0.1 M CF_3CO_2H at $[Cl^-] = 1.0$ M for ~2 h led to Cl_2 in 49% yield by thiosulfate titration. After the electrolysis, ~77% of the catalytic activity remained. It was totally restored by soaking in 0.1 M $HClO_4$ and then in water for several hours.[26] The oxidation of Cl^- was studied by rotating-disk voltammetry in 0.1 M $NaClO_4$ at pH 7.4 (0.05 M $H_2PO_4^-/HPO_4^{2-}$) at a film of $\Gamma = 1.1 \times 10^{-8}$ mol/cm^2 on an electrode of surface area 0.071 cm^2. Catalytic currents were independent of rotation rate over the range 0.1 mM ≤ $[Cl^-]$ ≤ 1 M. Under these conditions, catalytic currents (in parentheses) at the indicated $[Cl^-]$ were 1.6 mM (45 μA), 8.0 mM (105 μA), 40 mM (275 μA), 200 mM (475 μA), and 1.0 M (805 μA).

Discussion

Our results show that many of the features of the coordination chemistry of *cis*-$[Ru(bpy)_2(H_2O)_2]^{2+}$ are retained in films formed by oxidative or reductive electropolymerization. It is equally clear that the film environment plays its own role, in some cases in quite novel ways. One unusual observation came in the formation of the vinyl films by electrochemical reduction. Copolymerization of $[Ru(vbpy)_2(CO_3)]$ and $[Ru(vbpy)_3](PF_6)_2$ was required because the carbonato complex decomposed at the very negative potential required for direct reduction. It was incorporated into the growing network of poly-$[Ru(vbpy)_3]^{2+}$ even though its $E_{1/2}$ value for reduction was more negative than the electropolymerization potential by –0.3 V. The striking point was that the extent of its incorporation remained nearly constant at a ratio of ~$^1/_3$:~$^2/_3$ in films grown from solutions whose contents ranged from 1:1 to 1:9 $[Ru(vbpy)_3](PF_6)_2$:$[Ru(vbpy)_2(CO_3)]$. In other cases, such as coelectropolymerization of $[Ru(vbpy)_3](PF_6)_2$ and $[Os(vbpy)_3](PF_6)_2$, the contents of films follow the contents of the solution.[23a,24] The observation made here is remarkable and suggests that the carbonato complex may be uniformly dispersed throughout the film, occupying one-third of the available sites in the cross-linked polymeric network of poly-$[Ru(vbpy)_3]^{2+}$.

A second structural feature that appears in the films, which has important implications for their use in catalysis, is the apparent stabilization that occurs at oxidation state VI toward loss of bpy. As mentioned in the Introduction, oxidation of *cis*-$[Ru^{II}(bpy)_2(H_2O)_2]^{2+}$ to *cis*-$[Ru^{VI}(bpy)_2(O)_2]^{2+}$ is followed by rapid loss of bpy and formation of *trans,cis*-$[Ru^{VI}(bpy)(O)_2(OH)_2]$:[5]

$$cis\text{-}[Ru^{VI}(bpy)_2(O)_2]^{2+} + 2H_2O \rightarrow trans,cis\text{-}[Ru^{VI}(bpy)(O)_2(OH)_2] + bpyH^+ + H^+ \quad (14)$$

Even following repeated cycling through the wave at $E_{1/2} = 1.2$ V in the vinyl-based films, at potentials where Ru^{VI} is reached for the monomers in solution, there was no evidence for ligand loss. For poly-*cis*-$[Ru(pyr\text{-}bpy)_2(H_2O)_2]^{2+}$ the cyclic voltammetric evidence is less obvious for oxidation to Ru^{VI}, but repeated scans through the irreversible oxidation at $E_{p,a} \sim +1.3$ V gave no change in peak potential or current for the $Ru^{III/II}$ couple of poly-*cis*-$[Ru(pyr\text{-}bpy)_2(H_2O)_2]^{2+}$ on return scans. In fact, the

(26) The films poly-$[Ru(vbpy)_3]^{2+}$ and poly-$[Ru(pyr\text{-}bpy)_3]^{2+}$ are also electrocatalysts for the oxidation of Cl^- to Cl_2 under the same conditions. The catalytic currents are lower (by about one-tenth in comparable films) and time dependent. As shown by electrochemical measurements, oxidation induces loss of bpy over a period of time, which enhances the current level because the diaqua complex is produced.

(27) Samuels, G. J.; Meyer, T. J. *J. Am. Chem. Soc.* **1981**, *103*, 307.

characteristics of this wave were unaffected after holding the potential of the electrode at +1.3 V with an external solution at pH 1 for 24 h or after extended periods of electrocatalysis. From these observations, the *cis*-dioxo structure appears to be stabilized toward ligand loss in both the pyr-bpy and vbpy film environments.

The stability toward ligand loss in the films probably arises from their compact nature, which creates a kinetic barrier to the large-amplitude motions associated with loss of bpy. This is not an unreasonable suggestion. In solution the loss of bpy occurs by stepwise dissociation.[5] It would not be surprising if the opening of a bpy chelate were inhibited in the relatively rigid environment of the film.

Oxidative electropolymerization provides convenient access to poly-*cis*-$[Ru(pyr\text{-}bpy)_2Cl_2]$ and poly-$Ru[(pyr\text{-}bpy)_2(CO_3)]$, both of which are useful precursors to the bis(aqua) complex. The oxidative electropolymerizations were carried out at potentials that were sufficiently positive (+1.3 V) to destroy the conductivity of the polypyrrole network. The polypyrrole backbone still plays a role in defining the properties of the films. The repeat unit in films of poly-$[Ru(pyr\text{-}bpy)_2(CO_3)]$ is neutral, and yet, clear evidence for ClO_4^- anions was found in infrared spectra. They must be associated with cationic sites in the polypyrrole network. These sites are formed by partial oxidation of the polypyrrole.

Substitution. In water, stepwise solvolysis of Cl^- in *cis*-$[Ru(bpy)_2Cl_2]$ occurs, ultimately to give *cis*-$[Ru(bpy)_2(H_2O)_2]^{2+}$. In the pyrrole-based films, aquation of poly-*cis*-$[Ru(pyr\text{-}bpy)_2Cl_2]$ also occurs, and in a stepwise manner, to give poly-*cis*-$[Ru(pyr\text{-}bpy)_2(H_2O)_2]^{2+}$. But there is a profound difference in how aquation occurs in the film. Substitution begins only after an electrochemical cycle through the $Ru^{III/II}$ wave, and then not to completion. Each cycle induces substitution, but in time-dependent increments. The stepwise nature of the aquation is maintained, but a series of scans through the $Ru^{III/II}$ waves is required to achieve complete substitution.

This appears to be a pure film effect associated with the microenvironment surrounding the metal complexes. The properties of the complexes themselves are relatively unaffected, as shown by the similarities between the electrochemical and spectral properties for films and for solutions. The origin of the effect may lie in internal structural changes and/or changes in water content induced by oxidation. Oxidation to Ru^{III} increases charge and causes counterions to migrate into the films. The migration of anions may "open" the films toward diffusion of water, or the water molecules required for aquation may be waters of hydration drawn in with the anions. A related observation was made for poly-*cis*-$[Ru(pyr\text{-}bpy)_2(CH_3CN)_2]^{2+}$, where aquation was observed only after cycling through the $Ru^{III/II}$ couple.

A corollary that follows from these observations is the danger of attempting to utilize electrochemical monitoring of the films as a basis for establishing composition. In this case, the analytical measurement itself induces a chemical change and, by inference, significant changes in either internal structure or composition or both.

A related, substitution-based phenomenon, but one which occurs both in solution and in the films, was the stepwise, oxidatively induced loss of carbonate in $[Ru(bpy)_2(CO_3)]$ or poly-$[Ru(pyr\text{-}bpy)_2(CO_3)]$ in CH_3CN. In films of $^1/_3$poly-$[Ru(vbpy)_2(CO_3)]$-*co*-$^2/_3$poly-$[Ru(vbpy)_3]^{2+}$ the stepwise nature of the reaction is shown by the appearance of waves for the $Ru^{III/II}$ couples of poly-*cis*-$[Ru(vbpy)_2(HCO_3)(CH_3CN)]^+$ and poly-*cis*-$[Ru(vbpy)_2(CH_3CN)_2]^{2+}$ at $E_{1/2}$ = 0.76 and 1.33 V following oxidative scans through the $Ru^{III/II}$ wave at $E_{1/2}$ = 0.22 V. We have no experimental insight into the mechanism by which oxidation induces substitution and intend to explore this chemistry in further detail.

Electron-Transfer, pH, and Aging Effects. On ITO in 0.1 M $HClO_4$, the rate of oxidation of poly-*cis*-$[Ru(pyr\text{-}bpy)_2(H_2O)_2]^{2+}$ to poly-*cis*-$[Ru(pyr\text{-}bpy)_2(H_2O)(OH)]^{2+}$ appears to be limited by electron transfer at the film–electrode interface. The evidence for this comes from the kinetic studies. Oxidation of Ru^{II} to Ru^{III} (first kinetic run) occurs with k_{obs} = 0.65 s^{-1}. Oxidation of poly-$[Os^{II}(vbpy)_3]^{2+}$ to Os^{III} on ITO under the same conditions with the same technique occurs with $k_{obs} \sim 1$ s^{-1}.[23d] Oxidation of poly-$[Os^{II}(vbpy)_3]^{2+}$ to the Os^{III} complex in films on Pt soaked in CH_2Cl_2 is more rapid by a factor of $\sim 10^5$.[23a] The similarity between the two rate constants at ITO suggests rate-limiting interfacial electron transfer, perhaps due to a small number of surface states in the electrode. The kinetic measurements also revealed the existence of an aging effect for the poly-*cis*-$[Ru(pyr\text{-}bpy)_2(H_2O)_2]^{3+/2+}$ couple on ITO (but not glassy carbon) in 0.1 M $HClO_4$. The rate constant for oxidation of Ru^{II} to Ru^{III} decreased by 30-fold by the third kinetic run on the same film. There was no significant loss of the Ru complex, and for poly-$[Os(bpy)_3]^{2+}$ no aging effect was observed under the same conditions after several oxidation–reduction cycles.[23d] Presumably, complete oxidation of poly-*cis*-$[Ru^{II}(pyr\text{-}bpy)_2(H_2O)_2]^{2+}$ to poly-*cis*-$[Ru^{III}(pyr\text{-}bpy)_2(H_2O)_2]^{3+}$ causes a structural change at the polymer–ITO interface which further decreases the rate of interfacial electron transfer.

In poly-*cis*-$[Ru(pyr\text{-}bpy)_2(H_2O)_2]^{2+}$ on glassy carbon the pH dependence of the $Ru^{III/II}$ couple in solution is largely retained although there are some differences (Figure 5). However, unusual, pH-based kinetic effects do appear in the films which do not appear for couples that are pH independent. One is that the peak current for the $Ru^{III/II}$ couple in poly-*cis*-$[Ru(pyr\text{-}bpy)_2(H_2O)_2]^{2+}$ decreases as the pH is increased (Table II). Only peak currents are affected, $E_{1/2}$ for the couple is unaffected, and there is no evidence from scan rate dependent cyclic voltammograms for decreased rates of electron transfer.

Related pH effects have been observed in vinyl-based films.[28] This would appear to rule out protonation–deprotonation at the N atoms of the polypyrrole backbone as their origin (which is the case for the $Ru^{III/II}$ couple of $[Ru(bpy)_2(H_2O)(poly(4\text{-}vinylpyridine))]^{2+}$ in films of poly(4-vinylpyridine).[27] These effects can be explained by invoking kinetically distinct regions in the films and recalling the pH dependence of the $Ru^{III/II}$ couple (reaction 7a). Electrochemically "active" and "inactive" regions have been found for related $Ru^{III/II}$ couples in Nafion[29] and in chemically derivatived films of p-chlorosulfonated polystyrene.[30]

If the dynamics of proton transfer are different in different regions of the films, a portion of the electroactivity would be lost as the pH is increased.[29] In regions that are open to proton transport and have an *electron-transfer channel* to the electrode, oxidation of poly-*cis*-$[Ru^{II}(pyr\text{-}bpy)_2(H_2O)_2]^{2+}$ to poly-*cis*-$Ru^{III}(pyr\text{-}bpy)_2(H_2O)(OH)]^{2+}$ can occur with rapid proton equilibration. In regions that are closed to proton transport and isolated from the electrode, electron transfer could still occur, but indirectly by site to site hopping to sites in an electron–proton transfer channel.[30] Such "cross-domain" electron transfer would become increasingly unfavorable as the pH is increased. From the pH-dependent electrochemical data in Figure 5, $\Delta G^\circ \sim +0.2$ eV, at pH 5 for reaction 15.

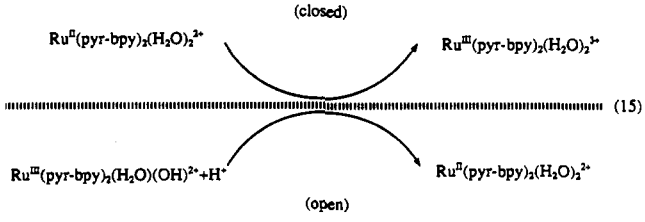

(28) Moss, J. Work in progress.
(29) Vining, W. J.; Meyer, T. J. *J. Electroanal. Chem. Interfacial Electrochem.* **1987**, *237*, 191.
(30) Surridge, N. A.; McClanahan, S. F.; Hupp, J. T.; Danielson, E.; Gould, S.; Meyer, T. J. *J. Phys. Chem.* **1989**, *93*, 304.

Table III. Summary of pH, Medium, and Aging Effects on Electrochemical and Electron-Transfer Properties

electrode	couple	medium	observation
		poly-*cis*-$[Ru(pyr\text{-}bpy)_2(H_2O)_2]^{2+}$ Film	
glassy carbon	$Ru^{III/II}$	0.1 M CF_3CO_2H compared to 0.1 M $HClO_4$	decreased peak currents
glassy carbon	$Ru^{III/II}$	varying pH	expected variation in $E_{1/2}$ with pH observed; decrease in peak current as the pH is increased
ITO	$Ru^{III/II}$	0.1 M $HClO_4$	rate-limiting interfacial electron transfer; decrease in k_{obs} by a factor of ~40 for oxidation of Ru^{II} to Ru^{III} after three kinetic cycles
glassy carbon	$Ru^{IV/III}$	0.1 M $HClO_4$	decrease in peak current compared to that for $Ru^{III/II}$
glassy carbon	$Ru^{IV/III}$	varying pH	variation of $E_{1/2}$ with pH as expected
glassy carbon	$Ru^{VI/V}$, $Ru^{V/IV}$	0.1 M $HClO_4$	irreversible oxidative wave observed but only on the first scan
		$^1/_3$poly-*cis*-$[Ru(pyr\text{-}bpy)_2(H_2O)_2]^{2+}$-*co*-$^2/_3$poly-$[Ru(vbpy)_3]^{2+}$ Film	
glassy carbon	$Ru^{III/IV}$	varying pH	$E_{1/2}$ varies with pH
glassy carbon	$Ru^{VI/V}$, $Ru^{V/IV}$, $Ru^{IV/III}$	varying pH	$E_{1/2}$ varies with pH
glassy carbon	$Ru^{VI/V}$, $Ru^{V/IV}$, $Ru^{IV/III}$	pH 5	peak currents decrease with scanning through these waves; evidence for only the $Ru^{VI/V}$ couple after a series of scans

A different kinetic effect was observed on multiple scans through the higher oxidation state couples. For poly-*cis*-$[Ru(pyr\text{-}bpy)_2(H_2O)_2]^{2+}$, waves for the $Ru^{III/II}$ and $Ru^{IV/III}$ couples were observed on the first scan and ill-defined waves for the $Ru^{V/IV}$ and $Ru^{V/VI}$ couples. The higher oxidation state couples did not appear on subsequent scans. For $^1/_3$poly-*cis*-$[Ru(vbpy)_2(H_2O)_2]^{2+}$-*co*-$^2/_3[Ru(vbpy)_3]^{2+}$, reasonably well-defined waves for all couples of poly-*cis*-$[Ru(vbpy)_2(H_2O)_2]^{2+}$ were observed on the first scan, but peak currents decreased on subsequent scans for the couples past $Ru^{III/II}$.

In both films, the aging effect may arise from local structural changes induced by conversion of the precursor carbonato or dichloro complexes, which are neutral, to the dicationic, diaqua complex. Aquation and addition of external anions (reactions 4 and 5) apparently produce the diaqua complex in a nonequilibrium environment with regard to electron–proton transfer.

Because of their complexity, a summary of the pH, medium, and aging effects is given in Table III.

Oxidation of Benzyl Alcohol and Chloride Ion. The kinetics of oxidation of benzyl alcohol by the pyrrole films were investigated as a preliminary to a larger study on electrocatalysis and possible sensor applications. The full scope of reactivity of the films toward organic and inorganic reductants, the fraction of sites that are catalytically active, and the roles of pH and medium effects remain to be established. The choice of benzyl alcohol as the reductant was a convenience. Its oxidation by *cis*-$[Ru^{IV}(bpy)_2(py)(O)]^{2+}$ had been investigated in detail.[9] Benzyl alcohol has also been used as a reductant in related electrocatalytic studies, and benzaldehyde is known to be the product.[4c,d,13i]

Significant oxidative catalytic currents appeared at poly-*cis*-$[Ru(pyr\text{-}bpy)_2(H_2O)_2]^{2+}$ with added benzyl alcohol, at pH 4.5, but only by scanning to potentials where the $Ru^{VI/V}$ and $Ru^{V/IV}$ couples appear. The active oxidant could be Ru^{VI} (as poly-*cis*-$[Ru(pyr\text{-}bpy)_2(O)_2]^{2+}$) or Ru^{V}. In the kinetic treatment of the catalytic currents, we chose to assume that the oxidant was Ru^{VI}, the catalytic couple $Ru^{VI/IV}$, and the mechanism as shown in eqs 9–12. Work in progress has shown that *trans*-$[Ru^{VI}(tpy)(O)_2(H_2O)]^{2+}$ is a facile oxidant of benzyl alcohol to give benzaldehyde and Ru^{IV}.[31]

The results of the kinetic study are consistent with the proposed mechanism. As shown by the absence of a rotation rate dependence in the rotating-disk experiments, the diffusion of benzyl alcohol to and within the film is sufficiently rapid so as not to be rate determining. The appearance of a saturation effect at high concentrations of benzyl alcohol and the linearity of the i_{lim}^{-1} vs $[C_6H_5CH_2OH]^{-1}$ plot are consistent with (1) rate-limiting oxidation of benzyl alcohol, (2) rate-limiting reoxidation of Ru^{IV} to Ru^{VI}, or (3) a competition between the two. From the magnitude of the $C_6H_5CH_2OH/C_6H_5CD_2OH$ kinetic isotope effect, (≥29), oxidation of benzyl alcohol is a major (and possibly the sole) contributor to the rate-determining step.

From the slope and slope to intercept ratio of the plot of i_{lim}^{-1} vs $[C_6H_5CH_2OH]^{-1}$, $k_{obs} = 0.37\ s^{-1}$ and $K_AK_p = 798\ M^{-1}$. The magnitude of K_AK_p suggests that benzyl alcohol concentrates in the film. The magnitude of the rate constant is impressive in pointing toward a high intrinsic reactivity toward oxidation of $C_6H_5CH_2OH$ by Ru^{VI} (and/or Ru^{V}) in the films. The half-time for a turnover from Ru^{VI} to Ru^{IV} at $[C_6H_5CH_2OH] = 1.0$ M is ~1.9 s. The second-order rate constant for oxidation of benzyl alcohol by *cis*-$[Ru^{IV}(bpy)_2(py)(O)]^{2+}$ is 2.4 $M^{-1}\ s^{-1}$ in 0.1 M $HClO_4$ at 25 °C,[9a] and that for oxidation by *trans*-$[Ru^{VI}(tpy)(O)_2(H_2O)]^{2+}$] is 13.3 $M^{-1}\ s^{-1}$ in 0.1 M $HClO_4$ at 25 °C.[31]

It is difficult to know what fraction of metal complex sites are involved in the electrocatalysis. Relative to 0.1 M $HClO_4$, about half the sites are inactive toward oxidation of Ru^{III} to Ru^{II} in the electrolysis medium, and well-defined waves for the higher oxidation state couples are not observed. By inference, the catalytic current is carried by only a small fraction of sites which are electroactive, making the reactivity of the active sites even more impressive.

It has been concluded that oxidation of benzyl alcohol by *cis*-$[Ru^{IV}(bpy)_2(py)(O)]^{2+}$ occurs by hydride transfer.[9a] An important piece of experimental evidence for this conclusion was the observation that the α,α'-(C–H/C–D) kinetic isotope effect in the oxidation of $C_6H_5CD_2OH$ relative to $C_6H_5CH_2OH$ is 50 in CH_3CN at 25 °C.[9a] From the ratio of peak currents for oxidation of $C_6H_5CH_2OH$ and $C_6H_5CD_2OH$ at 0.19 M, the isotope effect is ≥29 in the film, suggesting that the mechanism may be the same. The retention of kinetic isotope effects of this magnitude in the films suggests the possibility of using the film-based electrocatalysts for isotopic separation of H/D/T.

We have even less data on the oxidation of Cl^-. At pH 7.4, sustained catalytic, oxidative currents were observed. There is a dependence on $[Cl^-]$ but not on rotation rate. Controlled-potential electrolysis in acid gave Cl_2 as the product. The decrease in catalytic current over a sustained period appears to occur because of anation to give poly-*cis*-$[Ru(vbpy)_2(H_2O)Cl]^+$. Its formation would block oxidation to poly-*cis*-$[Ru^{VI}(vbpy)_2(O)_2]^{2+}$, since two bound H_2O molecules are required. The diaqua complex and the catalytic behavior can be restored by allowing the bound Cl^- to aquate. The appearance of this catalysis is significant in suggesting the possible use of suitably modified electrodes to generate Cl_2/HOCl in controlled microenvironments or in physiological systems where there is a ready supply of Cl^-.

Acknowledgment. A.R.G. thanks The University of North Carolina at Chapel Hill for her postdoctoral fellowship. We thank Professor R. W. Murray for helpful discussions. Financial support by the AROD under Grants DAAL03-88-K-0192 and DAAL03-90-G-0062 and by the NSF under Grant CHE-9203311 is gratefully acknowledged.

(31) Lebeau, E.; Binstead, R. Work in progress.